

# Zinc–Nucleic Acid Interaction

Shin Aoki†

Faculty of Pharmaceutical Sciences, Tokyo University of Science, 2641 Yamazaki, Noda 278-8510, Japan

Eiichi Kimura\*

Faculty of Integrated Arts and Sciences, Hiroshima University, 1-7-1 Kagamiyama, Higashi-Hiroshima 739-8521, Japan

Received June 20, 2003

## Contents

1. Introduction	769
2. Recognition of Thymines and Uracils by Zn <sup>2+</sup> –Cyclen Complex <b>2</b>	769
3. Recognition of Thymines and Guanines by Zn <sup>2+</sup> –Acridinylmethylcyclen <b>11</b>	771
4. Recognition of Thymidyl(3′–5′)thymidine (d(TpT)) by Bis(Zn <sup>2+</sup> –cyclen) Complexes and Thymidyl(3′–5′)thymidyl(3′–5′)thymidine (d(TpTpT)) by a Tris(Zn <sup>2+</sup> –cyclen) Complex	773
5. Effect of Bis(polyaromatic) Pendants of Zn <sup>2+</sup> Complexes on Thymine Recognition	774
6. Inhibition of Photo[2+2]cycloaddition of d(TpT) and Promotion of Photosplitting of the Cycloaddition Products by Bis(Zn <sup>2+</sup> –cyclen) Complexes	774
7. Selective Nucleobase Recognition in Single-Stranded Polynucleotides by Zn <sup>2+</sup> –Cyclen and Zn <sup>2+</sup> –Acridinylmethylcyclen	776
8. Recognition of Thymidine in Oligonucleotide by Zn <sup>2+</sup> –Acridinylmethylcyclen <b>11</b>	776
9. Selective Nucleobase Recognition in Double-Stranded Polynucleotides by Zn <sup>2+</sup> –Cyclen and Zn <sup>2+</sup> –Acridinylmethylcyclen, As Identified by T <sub>m</sub> Measurements	777
10. Footprinting Identification of the Zn <sup>2+</sup> –Cyclen Binding Sites in Natural DNA	778
11. Selective Interaction with TATA Box and Inhibition of TATA Binding Protein to TATA Box by Zn <sup>2+</sup> –Cyclen Complexes	781
12. Inhibition of in Vitro dT-rich DNA-Directed Transcription by Zn <sup>2+</sup> –Cyclen Complexes	782
13. Lipophilic Zn <sup>2+</sup> –Cyclen Complexes as Effective Carriers of AZT	783
14. Selective and Efficient Recognition of Thymidine Mono- (dTMP) and Diphosphate (dTDP) Nucleotides by the Ditopic Receptors Bis(Zn <sup>2+</sup> –cyclen) Complexes	784
15. Potent Inhibition of HIV-1 TAR RNA-Tat Peptide Binding by Zn <sup>2+</sup> Complexes	785
16. Summary	786
17. References	786

## 1. Introduction

Molecular recognition of DNA, RNA, and related biomolecules is responsible for a wide range of biochemical processes such as complementary base pairings in genetic information storage and transfer,<sup>1</sup> oligonucleotide recognition by ribozymes,<sup>2</sup> and actions of restriction enzymes,<sup>3</sup> etc. Recently, a number of artificial receptor molecules were synthesized for specific nucleic acid constituents (e.g., thymine (dT) or uracil (U)) to mimic such biochemical processes.<sup>4–9</sup> The molecular structure of these receptors was designed by mimicking naturally occurring noncovalent bonds such as hydrogen bonding, hydrophobic, or electrostatic interactions, etc. Unless they are in polymeric assemblies, these interactions are not as strong in aqueous solution.

In comparison, metal coordination, which normally is much stronger than the other noncovalent interactions, can serve as an extraordinarily strong binding element for biomolecular host–guest interactions in aqueous solution, as exemplified by *cis*-Pt(NH<sub>3</sub>)<sub>2</sub>Cl<sub>2</sub>.<sup>10</sup> Therefore, appropriate metal ions combined with well-designed ligands might have promising prospects in the development of new agents targeting nucleic acids.

Previously accumulated studies about the intrinsic chemical properties of Zn<sup>2+</sup> in biological environments demonstrated that the acidity of Zn<sup>2+</sup> can be finely tuned by complexation with macrocyclic polyamines such as 1,5,9-triazacyclododecane ([12]aneN<sub>3</sub>) and 1,4,7,10-tetraazacyclododecane ([12]aneN<sub>4</sub> or cyclen).<sup>11,12</sup> The distinctive acidity of Zn<sup>2+</sup> in the macrocyclic complexes was shown by the pK<sub>a</sub> values of the Zn<sup>2+</sup>-bound H<sub>2</sub>O from ca. 9 (for aquated Zn<sup>2+</sup> ion) to 7.3 and 7.9 for the Zn<sup>2+</sup>–[12]aneN<sub>3</sub> complex (**1a** ⇌ **1b**) and the Zn<sup>2+</sup>–cyclen complex (**2a** ⇌ **2b**), respectively, at 25 °C (Scheme 1).<sup>11,12</sup> Another manifestation of the enhanced reactivity of Zn<sup>2+</sup> was the 1:1 complexations of Zn<sup>2+</sup>–[12]aneN<sub>3</sub> **1** and Zn<sup>2+</sup>–cyclen **2** with deprotonated sulfonamides (see **3**) at neutral pH, despite the weak acidity of sulfonamides with pK<sub>a</sub> values of 7–10.<sup>13–15</sup>

## 2. Recognition of Thymines and Uracils by Zn<sup>2+</sup>–Cyclen Complex **2**

The strong binding of aromatic sulfonamides by the Zn<sup>2+</sup>–macrocyclic polyamines couples in neutral

\* Phone and fax: +81-824-24-6599. E-mail: ekimura@hiroshima-u.ac.jp.

† Phone and fax: +81-4-7121-3670. E-mail: shinaoki@rs.noda.tus.ac.jp.



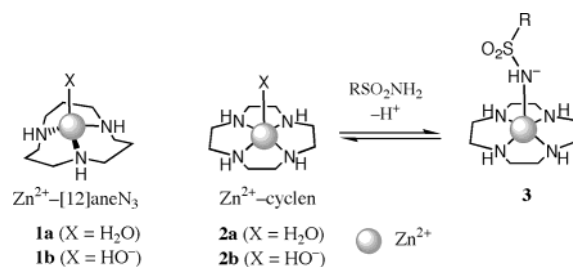
Shin Aoki was born in Sapporo, Japan, in 1964. He graduated from the University of Tokyo with his B.S. (1986), M.S. (1988), and Ph.D. (1992) degrees in pharmaceutical sciences under the supervision of Professor Kenji Koga. He started his academic career as an assistant professor at the University of Tokyo in 1990. Following postdoctoral positions with Professor Chi-Huey Wong at the Department of Chemistry, the Scripps Research Institute, he joined Professor Eiichi Kimura's research group in 1995 at the Faculty of Medicine, Hiroshima University, where he became an associate professor in 2001. In 2003, he became a professor at the Faculty of Pharmaceutical Sciences, Tokyo University of Science. He is a recipient of the Award of Japan Society of Coordination Chemistry for Young Scientists (1999), the AJINOMOTO Award in Synthetic Organic Chemistry, Japan (2001), and the Pharmaceutical Society of Japan Award for Young Scientists (2002). His major research interests are organic synthetic chemistry, bioinorganic chemistry, and supramolecular chemistry using metal complexes in aqueous solution.



Eiichi Kimura was born in Shizuoka, Japan, in 1938. He received his B.S. (1986) and M.S. (1988) degrees in pharmaceutical sciences from the University of Tokyo and his Ph.D. degree in chemistry from the University of North Carolina at Chapel Hill in 1967 under the supervision of Professor James P. Collman. Following postdoctoral positions at Syntax and the University of Chicago (with Professor Jack Halpern), he joined the Faculty of Medicine of Hiroshima University in 1970 and became a professor in 1978. He has contributed to macrocyclic chemistry, bioinorganic chemistry, medicinal chemistry, and supramolecular chemistry as the author or coauthor of over 240 scientific publications, reviews, and monographs. He was given the Chemical Society of Japan award in Inorganic Chemistry (1985), the 2nd Izatt–Christensen Award for Macrocyclic Chemistry (1992), and the Pharmaceutical Society of Japan Award (1996). He retired from Hiroshima University in 2002 and now is Professor Emeritus and Visiting Professor of Hiroshima University. He is currently the President of the Pharmaceutical Society of Japan.

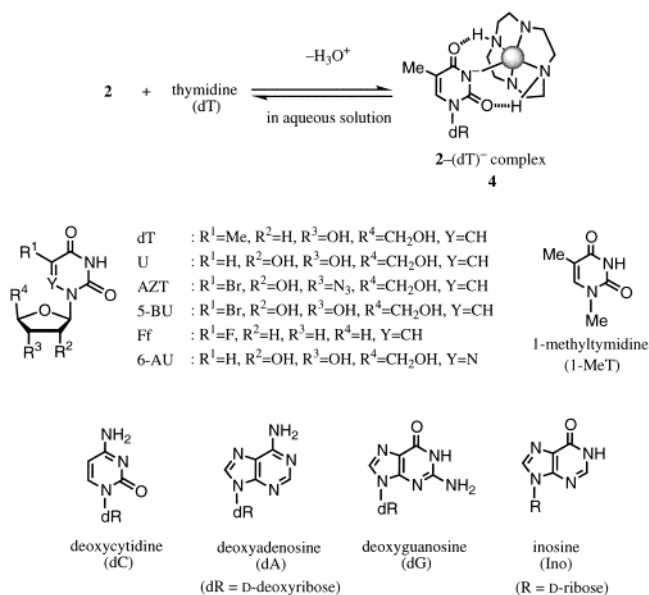
aqueous solution<sup>13–15</sup> has been applied to the novel molecular recognition of nucleobases, thymine (dT) and uracil (U), which possess similarly weak acidic protons at “imide” groups.<sup>16</sup> It was originally hypothesized that when Zn<sup>2+</sup>–cyclen complex **2** interacted with these “imide” functions, the acidic Zn<sup>2+</sup> might

### Scheme 1



replace the “imide” protons (such as sulfonamide protons) to yield a Zn<sup>2+</sup>–imide anion (N<sup>-</sup>) bond. Furthermore, the adjacent two “imide” carbonyls with developing negative charges might enhance the complexation by forming hydrogen bonds with the acidic NH hydrogens of the Zn<sup>2+</sup>–cyclen remaining at the complementary positions (see **4** in Scheme 2). Such

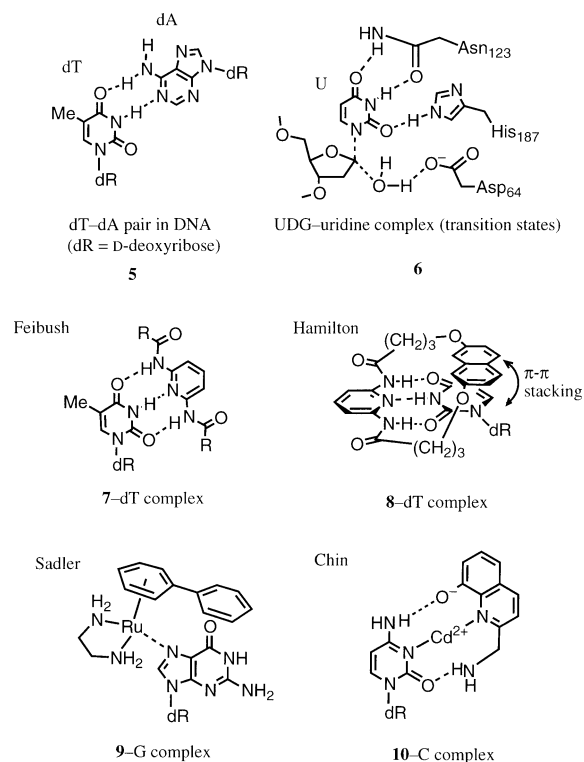
### Scheme 2



a coordination-involving motif should give different properties from previously known systems in biological A–dT or A–U systems in double-stranded nucleic acids (**5**), enzyme–nucleic acid complexes (such as *E. coli* uracil DNA glycosidase (UDG)–uridine complex **6**<sup>17</sup>), or earlier artificial complexes with organic receptors (**7**<sup>6</sup> and **8**<sup>7</sup>) in nonpolar solvents (Scheme 3).

Indeed, a strong association was first discovered in a crystalline 1:1 ternary complex **4** between the Zn<sup>2+</sup>–cyclen complex **2** and azidothymidine (AZT) in an aqueous solution at slightly alkaline pH of ~8.5.<sup>18</sup> An X-ray crystal structure analysis of the 1:1 ZnL–AZT complex revealed a distorted square pyramidal N<sub>5</sub>-coordinate structure indicating a strong coordinate interaction of Zn<sup>2+</sup> with the deprotonated “imide” N(3) anion (Figure 1).<sup>18</sup> The Zn<sup>2+</sup>–N(3) bond distance of 2.053(8) Å was shorter than the average Zn<sup>2+</sup>–NH (cyclen) bond distance of 2.153 Å. Although the distances were not as short as expected, the two indirect hydrogen bonds between the cyclen NH groups and the “imide” carbonyls were implicated by their proximities.

## Scheme 3



Potentiometric and spectrophotometric titrations of AZT, thymidine (dT), and related compounds in the presence of  $\text{Zn}^{2+}$ -cyclen ( $\text{ZnL}$ ) **2** proved the formation of a fairly stable 1:1 complex **4** with the deprotonated thymidine derivatives,  $\text{dT}^-$  ( $\log K = 5.6 \pm 0.1$ ,  $K = [\text{ZnL-dT}^-]/[\text{ZnL}][\text{dT}^-]$  ( $\text{M}^{-1}$ ) at  $25^\circ\text{C}$ , or  $\log K_{\text{app}} = 3.5 \pm 0.1$  at pH 8, where  $K_{\text{app}} = [\text{ZnL-dT}^-]/[\text{uncomplexed ZnL}][\text{uncomplexed dT}^-]$  ( $\text{M}^{-1}$ ), ( $\text{AZT}^-$  ( $\log K = 5.6 \pm 0.1$ )),  $\text{U}^-$  (uridine,  $5.2 \pm 0.1$ ), and ( $\text{Ff}^-$  (5-fluorouracil,  $4.6 \pm 0.1$ )) (Scheme 2).<sup>18</sup> Other nucleosides containing an amino group in place of the carbonyl oxygen of dT (i.e., 2-deoxyguanosine (dG)) or containing no acidic proton (i.e., 2-deoxyadenosine (dA) or 2-deoxycytidine (dC)) did not detectably bind to **2**, possibly due to the steric repulsion between the amino groups or to the lack of  $\text{N}^-$  anion formation. The linear relationship between  $\log K$  and  $\text{p}K_{\text{a}}$  of the nucleobases (Figure 2) supported the notion that the

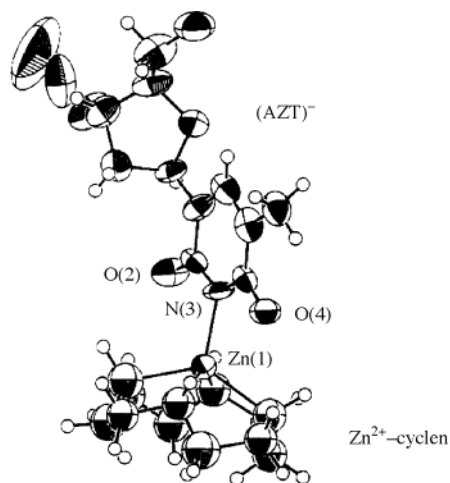


Figure 1. X-ray crystal structure of the **2**-(AZT)<sup>-</sup> complex.

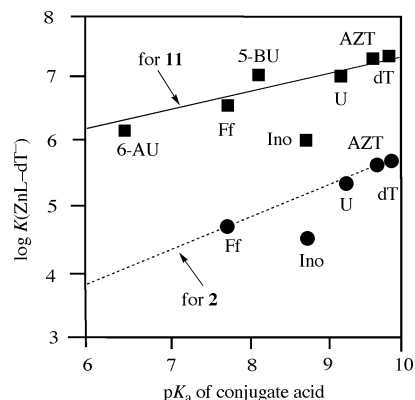


Figure 2. Plot of the complex ( $\text{ZnL-S}$ ) complexation constants for **2** (a) and **11** (b) with N(3)-for [or N(1)- for Ino] deprotonated nucleosides (S),  $\log K(\text{ZnL-S})$ , at  $25^\circ\text{C}$  against  $\text{p}K_{\text{a}}$  values for the nucleobase conjugate acids.

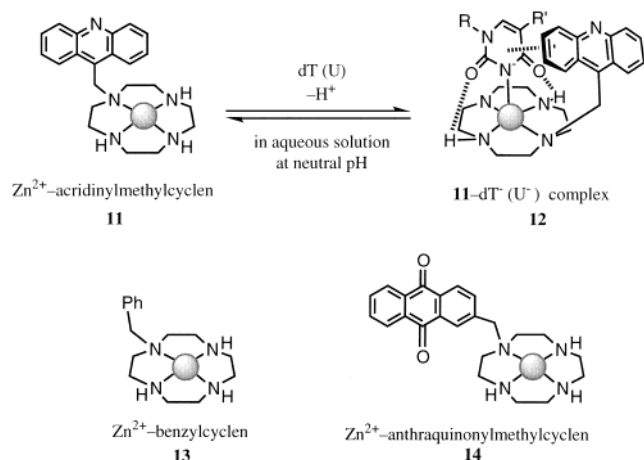
complex stability is governed by the basicity of the conjugate bases. By contrast, inosine, which lacks one carbonyl group at the C(2) position of dT, showed a slightly weaker affinity ( $\log K = 4.2 \pm 0.1$ ) and did not lie on the linear line. This indirectly proved that the two complementary hydrogen bonds between the “imide” carbonyl oxygens and the cyclen NH groups contribute appreciably to the stability of the ternary complexes. The  $\text{Zn}^{2+}$ -cyclen **2** had thus been discovered to be a new prototype of molecular recognition of the specific DNA/RNA nucleobase in aqueous solution.<sup>19,20</sup>

Other transition metal ions and their complexes<sup>21</sup> have been known to interact with nucleobases. The most nucleophilic site among nucleobases is N(7) of guanine, and this was a major target of these metal ions. For instance, the most classic anticancer drug, *cis*-Pt( $\text{NH}_3$ )<sub>2</sub>Cl<sub>2</sub>, most preferentially binds to guanine at the N(7) site.<sup>10</sup> Recently, Sadler's group reported that a Ru complex, [( $\eta^6$ -Bip)Ru(en)]<sub>2</sub> (Bip = biphenyl) **9**, binds to N(7) of guanine (Scheme 3), to N(7) and N(1) of inosine, and to N(3) of thymidine.<sup>22</sup> Chin et al. recently developed a Cd<sup>2+</sup> complex **10** as a new receptor for cytidine (C) in DMSO.<sup>23</sup> The zinc(II) ion with cyclen is thus a unique metal species that most preferentially recognizes the imide functionality of thymine (or uracil) bases. For other metal complexes which catalyze transesterification of nucleotides or their models<sup>24</sup> and nucleic acid-binding proteins such as zinc finger proteins,<sup>25</sup> see the references.

### 3. Recognition of Thymines and Guanines by $\text{Zn}^{2+}$ -Acridinylmethylcyclen **11**

Although a new type of dT (or U) recognition by  $\text{Zn}^{2+}$ -cyclen **2** was discovered, the dissociation constant  $K_{\text{d}}$  ( $= 1/K_{\text{app}}$ ) for the 1:1 **2**-dT<sup>-</sup> complex **4** was not functionally small enough with 0.79 mM at pH 7.4. To improve its dT recognition, the basic cyclen structure was modified with some functional groups attached as pendants that might provide additional nonbonding interaction with the nucleobase and/or ribose moieties. In the expectation of increased “multipoint” recognition, an acridine pendant was introduced onto the cyclen ring (acridinylmethylcyclen, **11** (see Scheme 4)).<sup>26</sup> It was hoped that the

## Scheme 4



polyaromatic acridine ring would make a supplemental  $\pi$ - $\pi$  stacking interaction with the aromatic nucleobases. Later, it was found that the pendant groups such as acridine became even more useful in working with double-stranded DNA.

Potentiometric pH titrations of the  $\text{Zn}^{2+}$ -acridinylmethylcyclen **11** were conducted in the presence of dT and its homologues to test the formation of more stable 1:1 complexes **12** (Scheme 4). The complexation constants  $K$  for **12** were all greater than those for the original **4** (see Figure 2), proving an additional binding force from the possible  $\pi$ - $\pi$  stacking interaction. The order of the affinities, dT ( $\log K = 7.2 \pm 0.1$ ), AZT ( $7.2 \pm 0.1$ ) > BU (5-bromouridine,  $7.0 \pm 0.1$ ) > U ( $6.9 \pm 0.1$ ) > Ff ( $6.6 \pm 0.1$ ) > AU (6-azauridine,  $6.3 \pm 0.1$ ), was consistent with that of the basicities of the conjugate base  $\text{N}(3)^-$ , as found with **2**. The dissociation constant  $K_d$  for **2**-dT $^-$  at pH 7.4 was  $8 \mu\text{M}$ . Moreover, a similar linear relationship between  $\log K$  and the  $\text{p}K_a$  values of the conjugated acids indicated that the  $\text{Zn}^{2+}$ - $\text{N}^-$  interaction dominated the recognition. The enhanced stability by  $\Delta \log K$  of 1.6–2.0 for **12** with respect to **4** may be translated into  $\Delta \Delta G^\circ = 2.2\text{--}2.7$  kcal/mol for the additional  $\pi$ - $\pi$  interaction in aqueous solution. Note that the  $\log K$  value for  $\text{Zn}^{2+}$ -benzylcyclen **13** with dT $^-$  was  $5.8 \pm 0.1$ , which was near  $5.6 \pm 0.1$  for **2**, implying that the phenyl ring attached to cyclen did not significantly affect the T $^-$  recognition. As for inosine, the affinity with **11** is again slightly smaller ( $\log K = 5.7 \pm 0.1$ ) than predicted from the amide  $\text{p}K_a$  value of 8.8, as found with **2** (Figure 2).<sup>26</sup> This again supports the notion that direct and/or indirect hydrogen bonding by the two carbonyl groups of the thymine derivatives serves to supplement the stability of the ternary complexes in aqueous solution.

The  $^1\text{H}$  nuclear magnetic resonance (NMR) titration (1 mM) of dT with **11** in  $\text{D}_2\text{O}$  at pD 8.4 exhibited a new set of signals for the thymine, anomeric sugar protons, and acridine protons with increasing intensity until an amount equivalent to **11** was reached.<sup>26</sup> This implies the kinetically inert nature of the 1:1 **11**-dT $^-$  complex **12** under the given conditions. Compare this with the earlier 1:1 **2**-dT $^-$  complex, which was kinetically labile in the NMR spectral behaviors. The upfield shifts of thymine and acridine protons in the **11**-dT $^-$  complex might suggest an appreciable

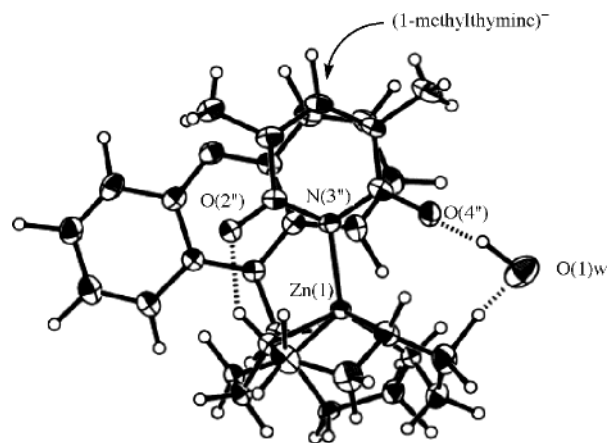


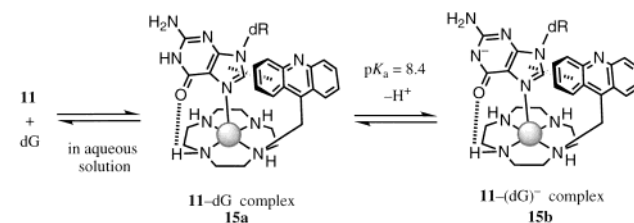
**Figure 3.** X-ray crystal structure of **11**-(1-methylthymine) $^-$  complex.

$\pi$ - $\pi$  stacking interaction. The extremely slow deuterium exchange of the two NH groups of the cyclen in the complex **12** was explained by the presence of the robust hydrogen bonds between the two NH groups and the two "imide" carbonyl oxygens even in the  $\text{D}_2\text{O}$  solution.

The X-ray crystal structure of the 1:1 ternary complex of **11** with N(3)-deprotonated 1-methylthymine (Figure 3) was consistent with the structure deduced from the solution behaviors. It was found that 1-methylthymine binds to  $\text{Zn}^{2+}$  in a distorted square pyramidal complex via  $\text{Zn}^{2+}$ -N(3')-deprotonated "imide" coordination with a short bond distance of 1.987-(4) Å.<sup>26</sup> All three NH groups of the cyclen rings were directed to the thymine base. The carbonyl oxygen O(2'') of the pyrimidine ring formed a hydrogen bond directly with a cyclen NH group, while the other carbonyl oxygen O(4'') bound indirectly via a water molecule to the other cyclen NH group. The pendant acridine stood upright face-to-face with the plane of the thymine with an interplane separation distance ranging from 3.285 to 3.419 Å (normally  $\sim 3.4$  Å for two cofacial aromatic interactions), indicating a well-arranged interfacial stacking between them. The overlapping positions of the acridine and the pyrimidine ring explain the aforementioned  $^1\text{H}$  NMR upfield shifts of protons on the periphery of the thymine base. The absence of any chemical shifts for the ribose protons suggests little influence from the acridine ring current.

The interactions of **11** with other nucleosides were examined by potentiometric pH titrations. dG was found to interact, although not as strongly as dT, with  $\log K$  values of  $4.1 \pm 0.1$  and  $5.0 \pm 0.1$  for the 1:1 complexes **15a** ( $K = [\text{ZnL-dG}]/[\text{ZnL}][\text{dG}]$  ( $\text{M}^{-1}$ )) and its deprotonated form **15b** ( $K = [\text{ZnL-dG}^-]/[\text{ZnL}][\text{dG}^-]$  ( $\text{M}^{-1}$ )), respectively (Scheme 5).<sup>26</sup> Since the

## Scheme 5



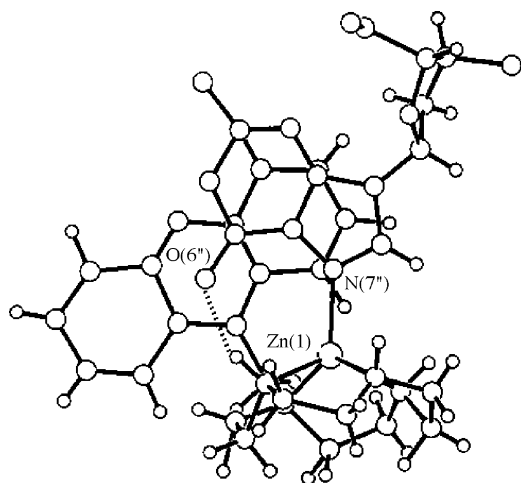


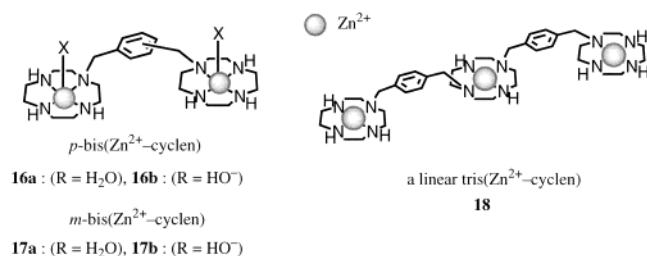
**Figure 4.** Interaction of **11** with 2-deoxyguanosine (dG) and the X-ray crystal structure of **11**-dG complex **15a**.

$Zn^{2+}$ -cyclen complex **2** showed little interaction with dG, the acridine-purine  $\pi$ - $\pi$  interaction must significantly assist the formation of **15a** ( $\rightleftharpoons$  **15b**). The  $pK_a$  value of 8.4 for **15a**  $\rightleftharpoons$  **15b** was supported by UV-spectrophotometric titration. The X-ray crystal structure of **15a** proved the  $\pi$ - $\pi$  stacking and  $Zn^{2+}$ -N(7'') coordination (Figure 4).<sup>26</sup> On the basis of the determined complexation constants for **11** with all the nucleosides, it was estimated that **11** (1 mM) binds with dT (71%) and dG (24%) in aqueous solution containing equivalent dT, dG, dA, and dC (each 1 mM) at pH 7.6 and 25 °C. Hence, **11** is selective for dT at physiological conditions.

Subsequently, a  $Zn^{2+}$ -cyclen complex appended with an anthraquinone **14** was synthesized, which formed a similarly stable 1:1 complex with dT<sup>-</sup> ( $\log K = 6.6 \pm 0.1$ ) and electrochemically responded to the complexation.<sup>27</sup> A new  $Zn^{2+}$  complex with 2,4-dinitrophenylcyclen also formed a 1:1 complex with dT<sup>-</sup> with  $\log K = 6.9 \pm 0.1$ .<sup>28</sup>

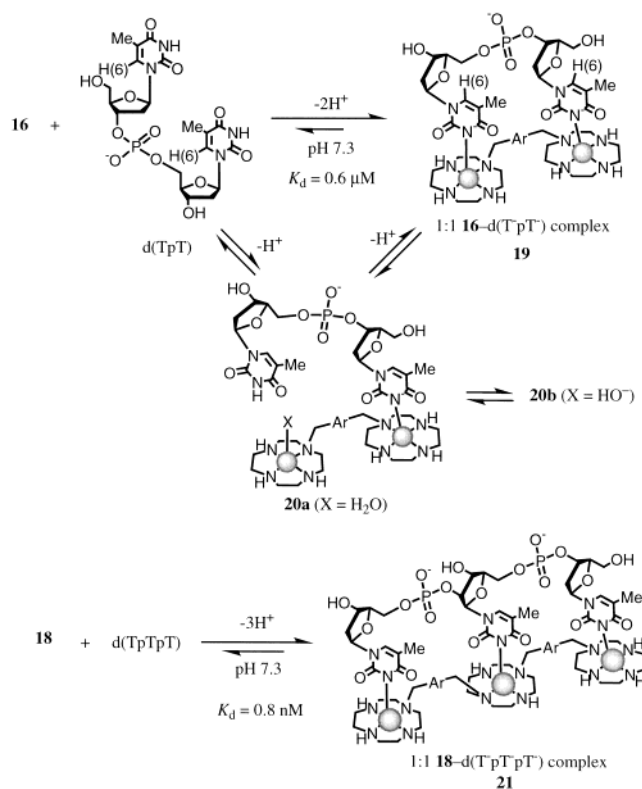
#### 4. Recognition of Thymidyl(3'-5')thymidine (d(TpT)) by Bis( $Zn^{2+}$ -cyclen) Complexes and Thymidyl(3'-5')thymidylyl(3'-5')thymidine (d(TpTpT)) by a Tris( $Zn^{2+}$ -cyclen) Complex

A dinucleotide thymidyl(3'-5')thymidine (d(TpT)) and a trinucleotide thymidyl(3'-5')thymidylyl(3'-5')thymidine (d(TpTpT)) were selectively and efficiently bound by *p*-(**16**)<sup>29</sup> and *m*-bis( $Zn^{2+}$ -cyclen) complex **17**<sup>30</sup> and a linear tris( $Zn^{2+}$ -cyclen) complex **18** to yield stable 1:1 complexes such as **19** and **21** at pH 7.4 in aqueous solution (Scheme 6).<sup>31</sup>



In a <sup>1</sup>H NMR titration of 5 mM d(TpT) with varying concentrations (0–10 mM) of **16** in D<sub>2</sub>O at 35 °C, pD

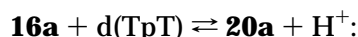
#### Scheme 6



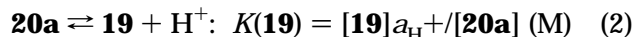
8.4, and  $I = 0.10$  (NaNO<sub>3</sub>), the signals of the two pyrimidine H(6) protons of d(TpT) exhibited an upfield shift from  $\delta = 7.65$  (5'-dT) and 7.68 (3'-dT) (for the numbering of H(6), see Scheme 6) to  $\delta = 7.51$  with peak broadening during the addition of one equivalent of **16**, implying higher electron density for the deprotonated thymidine groups.<sup>31</sup> No further change in the chemical shifts was seen above 5 mM of the titrants, indicating formation of an inert 1:1 complex **19**. It should be noted that the phosphodiester linker monoanion did not appear to interfere with the d(TpT)-**16** interaction.

The stoichiometric 1:1 complexation of d(TpT) with **16** was independently established by UV-spectrophotometric titrations of 0.5 mM d(TpT), in which a linear decrease in the UV absorption of d(TpT) at 267 nm was observed until equimolar amounts of **16** were reached, the decrease being due to a gradual formation of the deprotonated dT<sup>-</sup> with simultaneous  $Zn^{2+}$  complexations.

A quantitative study of the interaction of **16** (1.0 mM) with 2 equiv of dT (2.0 mM) or equimolar amount of dinucleotide d(TpT) (1.0 mM) was conducted by potentiometric pH titrations at 25 °C with  $I = 0.10$  (NaNO<sub>3</sub>). For the latter, the pH titration data (pH > 5) best fit the equilibria of the bis( $Zn^{2+}$ -cyclen)-d(TpT<sup>-</sup>) complex **20** (eq 1) and bis( $Zn^{2+}$ -cyclen)-d(TpT) **19** (eq 2) (Scheme 6) with  $\log K(\mathbf{20a})$  and  $\log K(\mathbf{19})$  values of  $-2.6 \pm 0.1$  and  $-5.5 \pm 0.1$ , respectively.<sup>31</sup>



$$K(\mathbf{20a}) = \frac{[\mathbf{20a}]_{\text{aH}}}{[\mathbf{16a}][d(\text{TpT})]} \quad (1)$$



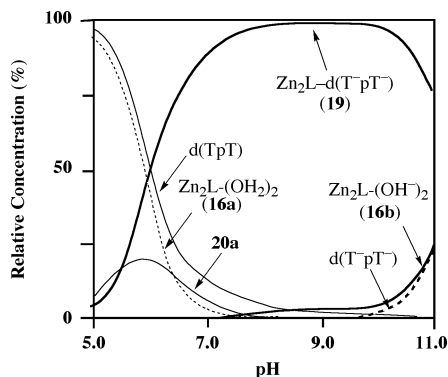
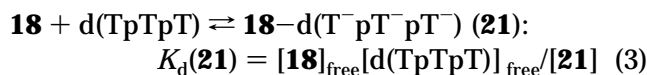


**Figure 5.** pH-Dependent species distribution for a mixture of 1 mM **16** and 1 mM d(TpT) at 25 °C with  $I = 0.10$  (NaNO<sub>3</sub>).

A species distribution diagram as a function of pH ( $= -\log a_{\text{H}^+}$ ) for an aqueous solution of 1 mM d(TpT) and 1 mM *p*-bis(Zn<sup>2+</sup>-cyclen) **16** is shown in Figure 5.<sup>31</sup> As expected from the above <sup>1</sup>H NMR and UV titration results, an almost stoichiometric formation of **19** is evident in the physiological pH region (i.e., more than 95% of **16** and d(TpT) are in the form of the 1:1 complex **19** in the pH range from 7 to 10). A dissociation constant  $K_d$  ( $= [\text{uncomplexed d(TpT)}] \cdot [\text{uncomplexed 16}]/[\text{19}]$ ) at pH 7.4 and 25 °C was estimated to be  $6.3 \times 10^{-7}$  M.

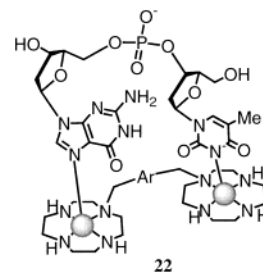
The stoichiometric 1:1 interaction of d(TpTpT) with tris(Zn<sup>2+</sup>-cyclen) **18** was also evidenced by a linear decrease in the UV absorption of d(TpTpT) until  $eq(\text{titrant}) = 1$  in pH 8 aqueous solution, implying the formation of 1:1 tris(Zn<sup>2+</sup>-cyclen)-d(T<sup>-</sup>pT<sup>-</sup>pT<sup>-</sup>) complex **21** (Scheme 6), whose FAB mass spectroscopic measurement revealed a major peak at  $m/z$  at 1763 with Zn isotopic peaks (1764, 1767, etc) for  $[(\text{T}^-\text{pT}^-\text{pT}^-)^{5-} \cdot \text{18}^{6+}]^+$  ( $m/z = 1762.81$ ). The potentiometric pH titrations determined that the dissociation constant,  $K_d(\text{21})$  (defined by eqs 3 and 4), at pH 7.4 and 25 °C with  $I = 0.10$  (NaNO<sub>3</sub>) was extremely small, at  $8.0 \times 10^{-10}$  M.<sup>31</sup>



$$[\text{d(TpTpT)}]_{\text{free}} = [\text{d(T}^-\text{pTpT)}]_{\text{free}} +$$

$$[\text{d(T}^-\text{pT}^-\text{pT}^-)]_{\text{free}} + [\text{d(T}^-\text{pT}^-\text{pT}^-)]_{\text{free}} \quad (4)$$

The *p*-bis(Zn<sup>2+</sup>-cyclen) **16** interacted far less favorably with other dinucleotides such as 2'-deoxyguanylylthymidine (d(GpT)), 2'-deoxycytidylylthymidine (d(CpT)), or 2'-deoxyadenylylthymidine (d(ApT)) at 25 °C with  $I = 0.10$  (NaNO<sub>3</sub>) in 10 mM HEPES buffer solution (pH 7.4).<sup>32</sup> The dissociation constant  $K_d$  of  $(1.3 \pm 0.1) \times 10^{-5}$  M for d(GpT) ( $= [\text{uncomplexed d(GpT)}][\text{uncomplexed bis(Zn}^{2+}\text{-cyclen)}]/[1:1 \text{ complex}]$ ) was obtained by isothermal calorimetric titrations. The complex structure **22** was proposed for the 1:1 **16**-d(GpT) association on the basis of the earlier G and T<sup>-</sup> binding modes with Zn<sup>2+</sup>-acridinylmethylcyclen. For the complexation of **16** with d(CpT) and d(ApT), accurate  $K_d$  values could not be obtained, primarily due to very weak interactions between **16** and these deoxydinucleotides.

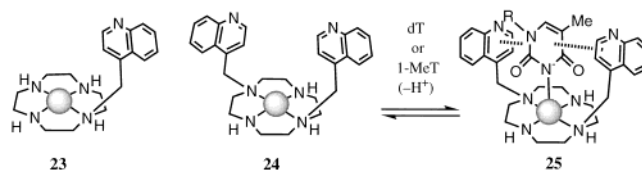


In conclusion, bis(Zn<sup>2+</sup>-cyclen) complexes **16** and **17** and tris(Zn<sup>2+</sup>-cyclen) **18** were shown to be a new type of sequence-selective nucleic acid binding ligand binding to d(TpT) and d(TpTpT), with  $K_d$  values on the order of micromolar and nanomolar, respectively, in aqueous solution at physiological pH.

### 5. Effect of Bis(polyaromatic) Pendants of Zn<sup>2+</sup> Complexes on Thymine Recognition

Bisintercalators occur naturally (e.g., triostin A, echinomycin (see section 10), and calzinophilin A) or artificially (e.g., bis(adenine) and ditercalinium).<sup>33</sup> Two aromatic groups such as naphthalene and quinoline rings have been attached to cyclen in the hope that they would sandwich the Zn<sup>2+</sup>-bound dT<sup>-</sup>. With respect to 6.8 for the 1:1 complex of Zn<sup>2+</sup>-mono((4-quinolyl)methyl) cyclen complex **23** with dT, a Zn<sup>2+</sup>-bis((4-quinolyl)methyl) cyclen complex **24** yielded a 1:1 complex **25** with  $\log K(\text{ZnL-dT}^-)$  of 7.7 (Scheme 7).<sup>33</sup> The apparent complexation constant for the 1:1 complex **25**,  $\log K_{\text{app}}(\mathbf{25})$ , at pH 8.0 and 25 °C was calculated to be 5.0, which is larger than that (4.7) for the **11**-dT<sup>-</sup> complex **12** (Scheme 4). The <sup>1</sup>H NMR titration of **24** with 1-methylthymidine (1-MeT) in varying D<sub>2</sub>O/CD<sub>3</sub>CN solution supported the double  $\pi$ - $\pi$  stacking of the two quinoline rings to contribute to greater stabilization of **25** in more polar environments.

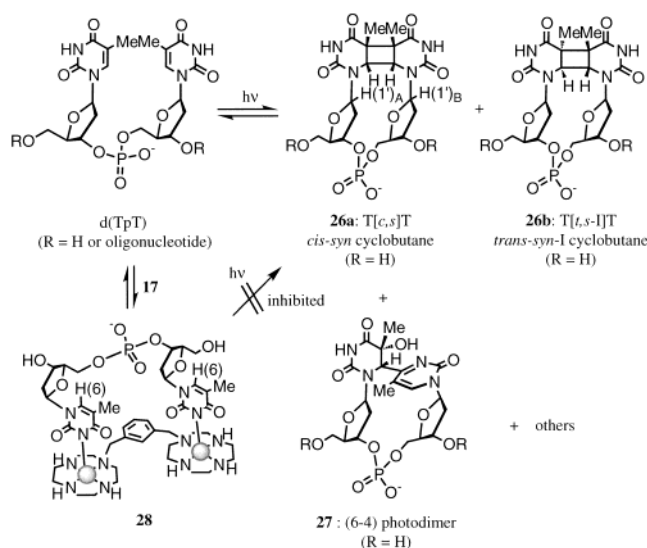
#### Scheme 7



### 6. Inhibition of Photo[2+2]cycloaddition of d(TpT) and Promotion of Photosplitting of the Cycloaddition Products by Bis(Zn<sup>2+</sup>-cyclen) Complexes

Exposure of cellular nucleic acids to UV radiation leads to a variety of lesions, which, if unrepaired, are potentially carcinogenic, mutagenic, or cytotoxic.<sup>34</sup> Among the known photoproducts of DNA, the major ones are *cis-syn*-(T[c,s]T) (**26a**) and *trans-syn*-I (T[t,s-I]T) (**26b**) cyclobutane thymine dimers and a pyrimidine(6-4)pyrimidone photodimer (**27**), all of which result from the photo[2+2]cycloaddition of two adjacent thymidylyl(3'-5')thymidine d(TpT) site (Scheme 8).<sup>35</sup> These base lesions induce base mutations in the p53 tumor suppressor gene<sup>36</sup> and even interfere in the interaction of DNA with proteins including RNA

## Scheme 8



polymerase II<sup>37</sup> or transcription factors.<sup>38</sup> Recent concerns about the depletion of the stratospheric ozone layer have led to efforts for the development of novel molecules that protect nucleic acids from UV exposure.<sup>39</sup> However, efficient methods of protecting nucleic acids from photodamage are still scarce.

It was supposed that the bis(Zn<sup>2+</sup>–cyclen) complexes **16** and **17** might be useful in prohibiting the photo[2+2]cycloaddition of d(TpT) by forming the inert and stable 1:1 complexes **19** (Scheme 6) and **28** (Scheme 8) and in promoting the reverse photo-splitting of the thymine dimers as an unprecedented prototype for protection of d(TpT) sites of DNA against UV light (Scheme 8).<sup>40</sup>

The results of the photoreaction of d(TpT) (0.2 mM in 10 mM Tris buffer at pH 7.6 ± 0.1 with  $I = 0.10$  (NaNO<sub>3</sub>) at 3–5 °C) in the absence and presence of mono(Zn<sup>2+</sup>–cyclen) **13**, bis(Zn<sup>2+</sup>–cyclen)'s **16**, and **17**, are displayed in Figure 6.<sup>40</sup> Curve a is a control reaction (quantum yield of  $(1.3 \pm 0.2) \times 10^{-2}$  at 266 nm). After irradiation for 3 h, 57% of d(TpT) disappeared and the photodimerization nearly reached equilibrium with the backward photosplitting reac-

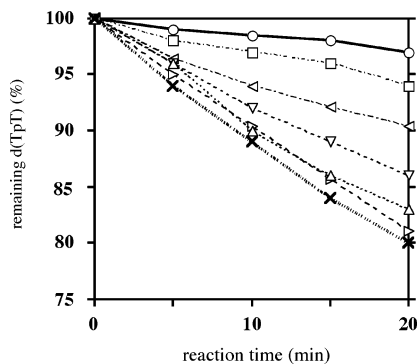
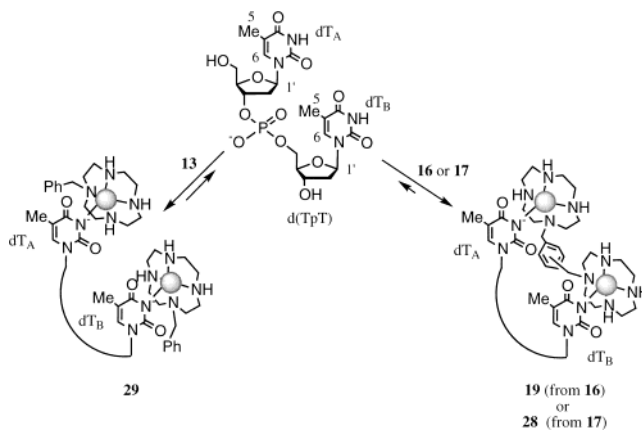


**Figure 6.** Effect of Zn<sup>2+</sup>–cyclen complexes or pH on the photodimerization of d(TpT) at 3–5 °C: (a) 0.2 mM d(TpT) at pH 7.6; (b) 0.2 mM d(TpT) + 0.2 mM Zn<sup>2+</sup>–benzylcyclen **13** at pH 7.6; (c) 0.2 mM d(TpT) + 0.4 mM **13** at pH 7.6; (d) 0.2 mM d(TpT) + 0.2 mM *p*-bis(Zn<sup>2+</sup>–cyclen) **16** at pH 7.6; (e) 0.2 mM d(TpT) + 0.2 mM *m*-bis(Zn<sup>2+</sup>–cyclen) **17** at pH 7.6; (f) 0.2 mM d(TpT) at pH 9.3 (10 mM Na<sub>2</sub>CO<sub>3</sub>–NaHCO<sub>3</sub>); and (g) 0.2 mM d(TpT) at pH 11.4 (10 mM Na<sub>2</sub>CO<sub>3</sub>–NaOH).

## Scheme 9

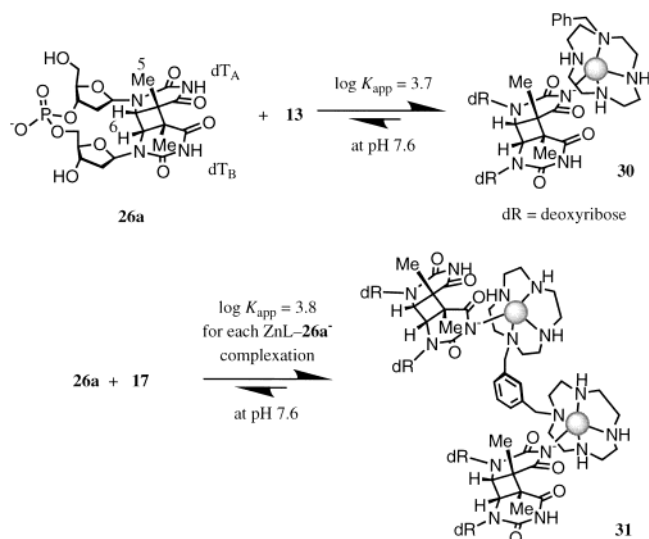


tion. Curves b and c show that the addition of **1** and **2** equiv of the mono(Zn<sup>2+</sup>–cyclen) derivative **13** was somewhat effective in reducing the rate of photodimerization. In contrast, the dimeric zinc(II) complexes, *p*-bis(Zn<sup>2+</sup>–cyclen) **16** (curve (d)) and *m*-bis(Zn<sup>2+</sup>–cyclen) **17** (curve (e)), more effectively reduced the rates of photodimerization (by 85% and 70% of the control reaction, respectively) than the 2 equiv of **13** (curve (c)). The presence of 1 mM ZnSO<sub>4</sub> without cyclen ligands did not affect the reaction rate. The presence of 1 mM Hg<sup>2+</sup> ion reduced the reaction rate to 34% of the control reaction, while the presence of Mn<sup>2+</sup> and Ni<sup>2+</sup> (both 1 mM) had no effect.

Calculation based on the  $K_d$  values indicated that the 1:1 complexes such as **28** (from d(TpT) and **17**) were formed in ca. 95% yield at [d(TpT)] = [*m*-bis(Zn<sup>2+</sup>–cyclen)] = 0.2 mM, pH 7.6, and 25 °C (Scheme 9). This means that 95% of d(TpT) is in the dianionic form to bind with two zinc(II) cations. At [d(TpT)] = 0.2 mM and [bis(Zn<sup>2+</sup>–cyclen)] = 0.4 mM, over 99% of d(TpT) should be in the complex form. Under the same conditions, d(TpT) (0.2 mM) formed a 1:2 complex **29** with a monomeric **13** (0.4 mM) in only 4% yield. To break down the inhibitory effects of Zn<sup>2+</sup>–cyclen into the electronic factor (anionic imide formation) and the steric factor, control reactions without zinc(II) complexes were conducted at pH 9.3, (curve (f) in Figure 6) and pH 11.4 (curve (g) in Figure 6), where 4% and 95% of d(TpT) are double-deprotonated species d(T<sup>–</sup>pT<sup>–</sup>), respectively, on the basis of the  $pK_a$  values ( $pK_{a1} = 9.5$  and  $pK_{a2} = 10.2$  at 25 °C). The photoreaction was only slightly inhibited at pH 9.3 (curve (g)) but greatly inhibited at pH 11.4, suggesting that the enhanced dT deprotonation at pH 7.6 by the strong Zn<sup>2+</sup> complexation contributed to the inhibition. The rest of the inhibition probably came from the steric factor caused by the bis(Zn<sup>2+</sup>–cyclen) complexation, which keeps the two dT moieties apart.<sup>40</sup>

The lifetime of a triplet state of pyrimidines has been estimated to be ca.  $10^{-5}$  s,<sup>38</sup> which is shorter with respect to the lifetime estimated by the <sup>1</sup>H NMR study of the **17**–d(T<sup>–</sup>pT<sup>–</sup>) complex **28** ( $10^{-3}$ – $10^{-2}$  s). Therefore, it was concluded that the two thymine rings were separated from each other by the two Zn<sup>2+</sup>–cyclen moieties spaced by a xylene unit (10 Å) for a period long enough to prevent close contact for photo[2+2]cycloaddition via a short-lived triplet state.

## Scheme 10



The calorimetric titrations indicated that the thymine photodimer **26a** formed a 1:1 complex **30** with **13** and a 1:2 complex **31** with **17** in aqueous solution at neutral pH, as shown in Scheme 10.<sup>40</sup> The photosplitting reaction of a thymine dimer **26a** was tested in the absence and presence of **13** and **17** at pD 8.0. Figure 7 displays the time course of the recovery of d(TpT) from the thymine photodimer (0.2 mM) in the absence and presence of a monomeric **13** (0.2 and 0.8 mM) and *m*-dimer **17** (0.4 mM) at pH 7.6 (in 5 mM Tris buffer (pH 7.6 with  $I = 0.1$  (NaNO<sub>3</sub>))). The reactions were followed by an increase in UV absorption at 266 nm. Curves b, c, and d display the results of the photosplitting of the thymine photodimer **26a** (0.2 mM) in the presence of 0.2 mM **13**, 0.8 mM **13**, and 0.4 mM **17**, respectively. The initial photosplitting rates were 1.7 times faster than that of the control reaction (curve a). After a few minutes, the rates of the recovery of d(TpT) were in the order of  $d > c > b > a$ . The yield of the photosplit d(TpT) in the presence of 0.4 mM **17** after 2 h was ca. 90%, which nearly agreed with the equilibrium ratio attained from the photodimerization reaction. In addition, **17** was shown to inhibit the photodimerization of the d(TpT) segments in poly(dT) and to promote the

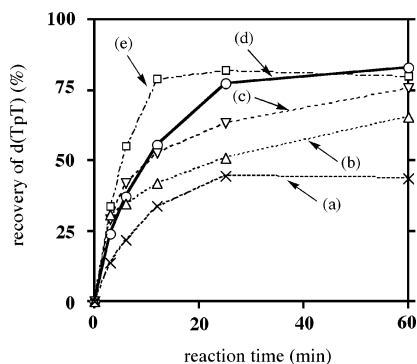


**Figure 7.** Effect of Zn<sup>2+</sup>-cyclen complexes or pH on the photosplitting of T[c,s]T **26a** at 3–5 °C: (a) 0.2 mM **26a** at pH 7.6, (b) 0.2 mM **26a** + 0.2 mM **13** at pH 7.6, (c) 0.2 mM **26a** + 0.8 mM **13** at pH 7.6, (d) 0.2 mM **26a** + 0.4 mM **17** at pH 7.6, and (e) 0.2 mM **26a** at pH 13.6.

reverse photosplitting of the photodimerized poly(dT), as evidenced by UV spectra.

### 7. Selective Nucleobase Recognition in Single-Stranded Polynucleotides by Zn<sup>2+</sup>-Cyclen and Zn<sup>2+</sup>-Acridinylmethylcyclen

Previously, interaction of Zn<sup>2+</sup>-cyclen complex **2** with phosphodiester monoanions was not found in neutral aqueous solution.<sup>11</sup> It was thus likely that the Zn<sup>2+</sup>-cyclen complexes would first recognize the thymine (or uracil) part in polynucleotides. In the UV titration of poly(U) (100 μM in terms of the phosphate or uracil group) with **2** (0–500 μM) in pH 7.6 buffer solution at 25 °C, the absorption maximum λ<sub>max</sub> (at 257 nm) of poly(U) linearly decreased with an increase in the concentration of **2**. Previously, almost the same UV titration spectrum was obtained for uridine nucleoside (U) (100 μM) with **2** (0–500 μM).<sup>18</sup> It was implied that **2** binds to U<sup>-</sup> in poly(U) and nucleoside in a similar order.<sup>42</sup>

An intuitive observation of H<sup>+</sup> release (i.e., drop in pH) in mixing Zn<sup>2+</sup>-acridinylmethylcyclen complex **11** (100 μM) with poly(dT) (10 μM per base) in pH 7.4 unbuffered solution provided good evidence for the interaction of **11** with T<sup>-</sup> in poly(dT).<sup>43</sup> Moreover, by measuring the released [H<sup>+</sup>] (= 6.8 μM), one could roughly estimate the 1:1 complexation constant  $K_{app} (= [ZnL-(dT^-)] / [ZnL]_{free} [dT^-]_{free})$  in poly(dT) of  $(2.4 \pm 0.1) \times 10^4 \text{ M}^{-1}$ , which was close to the  $K_{app} (= [ZnL-dT^-] / [ZnL]_{free} [dT^-]_{free})$  value of  $(3.6 \pm 0.1) \times 10^4 \text{ M}^{-1}$  (at 25 °C, pH 7.4), obtained from the potentiometric pH titration for the 1:1 **11**-nucleoside thymidine complex.

### 8. Recognition of Thymidine in Oligonucleotide by Zn<sup>2+</sup>-Acridinylmethylcyclen 11

Interaction of the Zn<sup>2+</sup>-acridinylmethylcyclen complex **11** at various concentrations with a single-stranded octanucleotide (1.0 mM), d(G<sub>1</sub>T<sub>2</sub>G<sub>3</sub>A<sub>4</sub>C<sub>5</sub>G<sub>6</sub>C<sub>7</sub>C<sub>8</sub>), was examined by <sup>1</sup>H NMR titrations at pD 8.4 and 5 °C (Figure 8).<sup>43</sup> When 0.6 mM **11** was added, the 50% intensity of the CH<sub>3</sub> signal at δ 1.61 of the original T<sub>2</sub> (see Figure 8a) decreased and a new peak appeared at δ 1.73 with 45% intensity (Figure 8b), which was assigned to the CH<sub>3</sub>(5) group of **11**-bound (T<sub>2</sub>)<sup>-</sup>. In the presence of 1.0 mM **11**, 80% of d(G<sub>1</sub>T<sub>2</sub>G<sub>3</sub>A<sub>4</sub>C<sub>5</sub>G<sub>6</sub>C<sub>7</sub>C<sub>8</sub>) was bound to **11** at the T<sub>2</sub> base (Figure 8c). When excess amounts of **11** (1.2 mM) were added, 90% of d(G<sub>1</sub>(**11**-T<sub>2</sub>)G<sub>3</sub>A<sub>4</sub>C<sub>5</sub>G<sub>6</sub>C<sub>7</sub>C<sub>8</sub>) was formed and the CH<sub>3</sub>(5) signal of the original T<sub>2</sub> disappeared (Figure 8d). When 2 mM **11** was added, the CH<sub>3</sub>(5) signal of the **11**-bound (T<sub>2</sub>)<sup>-</sup> decreased to 30% and the aromatic protons for the octanucleotide broadened, suggesting that the excess **11** randomly interacted with the other bases (Figure 8e). It was concluded that at [**11**] < 1.2 mM, the Zn<sup>2+</sup>-acridinylmethylcyclen complex **11** preferentially bound to the dT in d(GTGACGCC) (1 mM) regardless of the presence of three G bases.



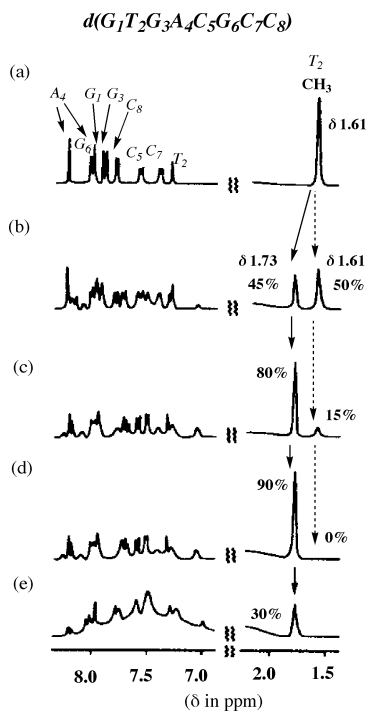


**Figure 8.**  $^1\text{H}$  NMR spectra of a single-stranded octanucleotide,  $d(\text{GTGACGCC})$  (1 mM) in the absence (a) and presence of 0.6 mM (b), 1.0 mM (c), 1.2 mM (d), and 2.0 mM (e) of **11** at pD 8.4 and 5 °C.

### 9. Selective Nucleobase Recognition in Double-Stranded Polynucleotides by $\text{Zn}^{2+}$ -Cyclen and $\text{Zn}^{2+}$ -Acridinylmethylcyclen, As Identified by $T_m$ Measurements

It is interesting to see whether the selective binding of  $\text{Zn}^{2+}$ -cyclen complexes to dT or U leads to the perturbation of a double-stranded poly(dA)·poly(dT) or poly(A)·poly(U) structure. When double-stranded DNA/RNA polymers were heated slowly, the double helix “melts” to each single component, which is detected by the sudden “hypochromic effect” in the UV absorptions of the nucleobase. The midpoint temperature of this transition corresponds to the melting temperature ( $T_m$ ) of the double-helical DNA/RNA polymers. Cations (e.g.,  $\text{Na}^+$ ,  $\text{Mg}^{2+}$ ,  $\text{Ca}^{2+}$ , and protonated spermidine),<sup>44</sup> DNA-binding organic compounds (e.g., distamycin and netropsin),<sup>45</sup> or intercalating agents (e.g., ethidium bromide and acridines)<sup>46</sup> normally raise  $T_m$  by stabilizing double-stranded DNA/RNA. Conversely, if a DNA/RNA double helix was destabilized, the melting temperature would be lowered.

Thermal melting curves for poly(A)·poly(U) (100  $\mu\text{M}$  base) in the absence and presence of varying concentrations of monomeric  $\text{Zn}^{2+}$ -cyclen derivatives (**2**, **11**, and a naphthylmethylcyclen complex **32**) and a dimeric **16** were determined by following the absorption changes at 260 or 270 nm as a function of temperature in a buffer solution (pH 7.6, 5 mM Tris-HCl and 10 mM NaCl) (Figure 9).<sup>42</sup> In the absence of  $\text{Zn}^{2+}$ -cyclen complexes ( $r = 0$ , where  $r = [\text{Zn}^{2+}\text{-cyclen}]/[\text{U in poly(U)}]$ ), the melting transition occurred at  $T_m$  (= 41.5 °C) (see Figure 9a–d). Upon increasing the concentration of the  $\text{Zn}^{2+}$ -cyclen complexes (i.e.,  $r$  was increased),  $T_m$  generally shifted

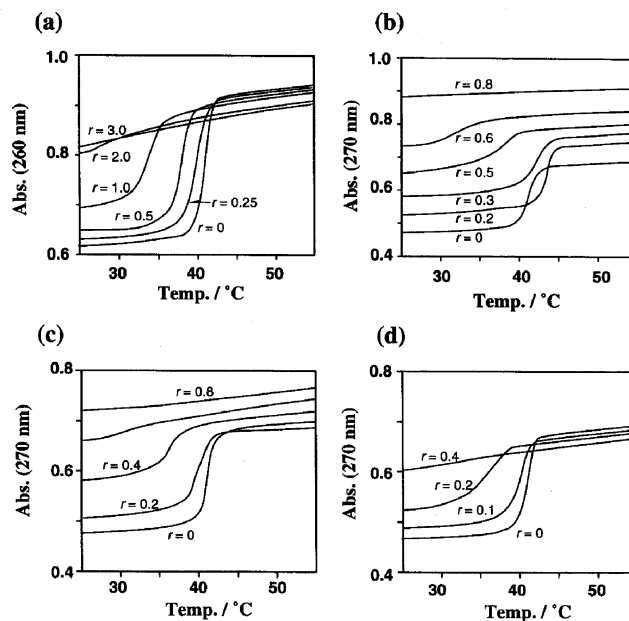
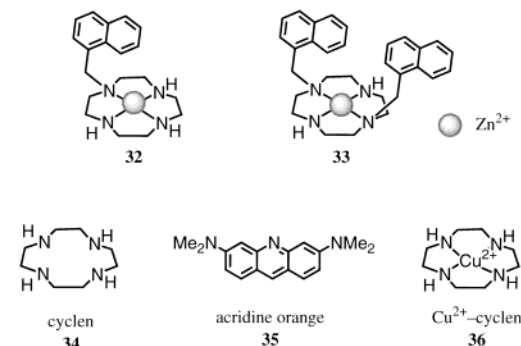


**Figure 9.** Melting curves for poly(A)·poly(U) in the presence of different concentrations ( $r$ ) of  $\text{Zn}^{II}$ -cyclen complexes **2** (a), **11** (b), **32** (c), and **16** (d) at pH 7.6 (5 mM Tris-HCl buffer) with 10 mM NaCl.

to a lower temperature and reduced hypochromicity was seen at 25 °C. These facts indicate that the A–U base pairs are disrupted or destabilized by all the  $\text{Zn}^{2+}$ -cyclen complexes that were tested. The disappearance of the hypochromic effect at 25 °C means that the helix disruption even occurred at 25 °C. The  $T_m$  break disappeared with 150  $\mu\text{M}$  ( $r = 3.0$ ) **2** (Figure 9a), 40  $\mu\text{M}$  ( $r = 0.8$ ) **11** (Figure 9b), 30  $\mu\text{M}$  ( $r = 0.6$ ) **32** (Figure 9c), and 10  $\mu\text{M}$  ( $r = 0.4$ ) **16** (Figure 9d). Therefore, among the four  $\text{Zn}^{2+}$  complexes which were tested, the *p*-bis( $\text{Zn}^{2+}$ -cyclen) **16** was considered the most powerful in terms of breaking the poly(A)·poly(U) double strand.

A mixed effect of **11** on the poly(A)·poly(U) double strand was found (Figure 9b).<sup>42,43</sup> Up to  $r = 0.3$ , **11** stabilized the double-stranded poly(A)·poly(U) ( $T_m = 41.5$  °C  $\rightarrow$  43.5 °C). However, at  $r > 0.3$ , increasing the concentration of **11** lowered  $T_m$ , and at  $r = 0.8$  (40  $\mu\text{M}$ ) the  $T_m$  break disappeared. For reference, the acridinylmethylcyclen ligand, which is chiefly in a diprotonated form ( $\text{L}\cdot\text{H}_2^{2+}$ ) in pH 7.6, simply raised  $T_m$  (e.g.,  $\Delta T_m = +8$  °C at  $r = 0.8$ ). Furthermore, other references such as cyclen ligand **34** (as a diprotonated species), acridine orange **35**, and  $\text{Cu}^{2+}$ -cyclen complex **36** all stabilized the double-



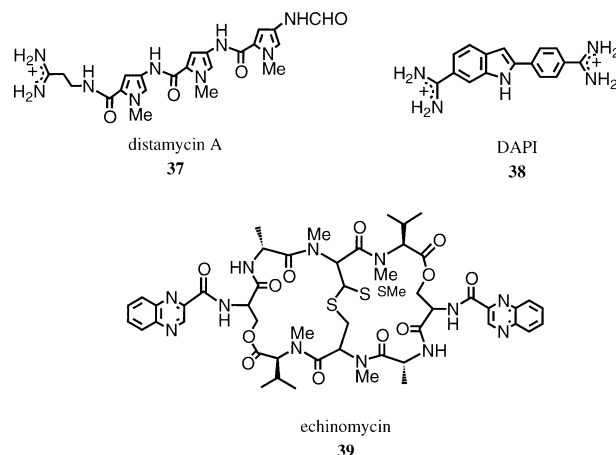
strand structure of poly(A)·poly(U) ( $\Delta T_m = +5.5$  °C for **34**,  $+18.5$  °C for **35**, and  $+6.5$  °C for **36** at  $r = 1.0$ ). The stabilization effects of these reference compounds were explained by the fact that they interact with the double-stranded polyanionic nucleic acid simply as polycations to diminish the repulsive negative charges on the phosphate backbone of the duplex.

From these results, it was concluded that all  $Zn^{2+}$ -cyclen complexes penetrate the core of the double strands to directly bind to the N(3)-deprotonated uracil bases in double-stranded poly(A)·poly(U) to denature the double-stranded structure.

### 10. Footprinting Identification of the $Zn^{2+}$ -Cyclen Binding Sites in Natural DNA

The detailed interaction sites of the  $Zn^{2+}$ -cyclen complexes, **11**, **23**, **24**, **32**, and **33**, in native DNA were identified by a biochemical DNA footprinting technique.<sup>47–50</sup> The binding sites of these  $Zn^{2+}$ -cyclen complexes in 5'-<sup>32</sup>P labeled DNA fragments (arbitrary A–T rich 150 bp) from plasmid pUC19 were first analyzed by a DNase I footprinting method for the upper and lower strands (Figure 10). The patterns of the DNase I digestion with or without the  $Zn^{2+}$ -

cyclen complexes, along with the DNA base sequence, are shown for the upper and lower strands (Figure 11). For references, typical AT binders, distamycin A **37**<sup>51</sup> (at a concentration range of 0.625–1.25  $\mu$ M) and DAPI **38**<sup>52</sup> (1.25–2.5  $\mu$ M), and a typical GC binder, echinomycin **39**<sup>53</sup> (2.5–5  $\mu$ M), were tested side by side on the same gel plate.



As shown in Figure 10, the regions protected by the  $Zn^{2+}$ -cyclen derivatives are associated with the

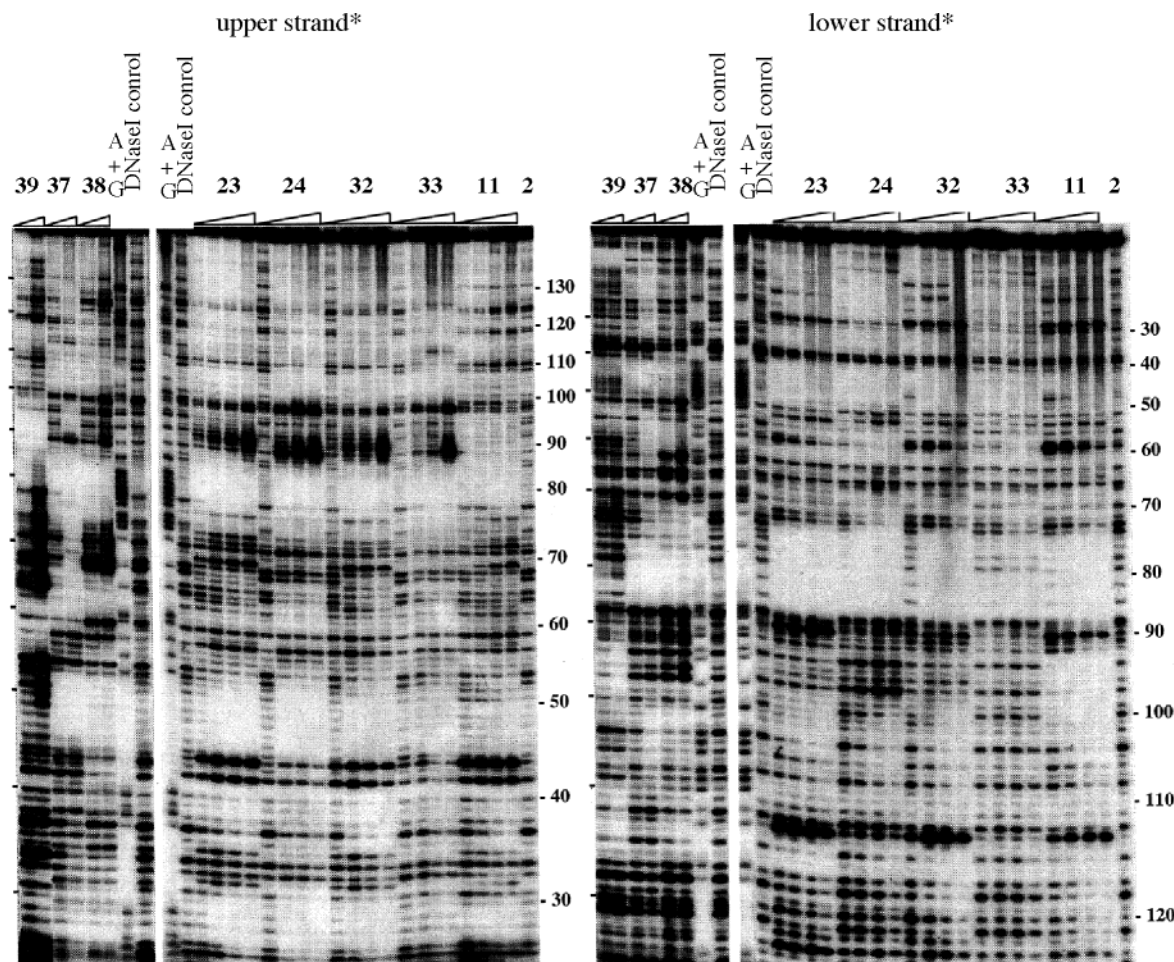


**Figure 10.** DNase I footprinting of 150 bp DNA treated with **39** (0.625 and 1.25  $\mu$ M), **37** (1.25 and 2.5  $\mu$ M), **38** (2.5 and 5  $\mu$ M), **23** (30, 40, 50, and 60  $\mu$ M), **24** (7.5, 10, 12.5, and 15  $\mu$ M), **32** (20, 30, 40, and 50  $\mu$ M), **33** (5, 7.5, 10, and 12.5  $\mu$ M), **11** (5, 7.5, 10, and 12.5  $\mu$ M), and **2** (100  $\mu$ M). The asterisk indicates which strand bears the 5'-<sup>32</sup>P label (upper strand or lower strand shown in Figure 10). The lane labeled "A+G" represents the Maxam–Gilbert sequencing marker specific for A and G. The lane labeled "DNase I control" represents DNA digested with DNase I without binders.

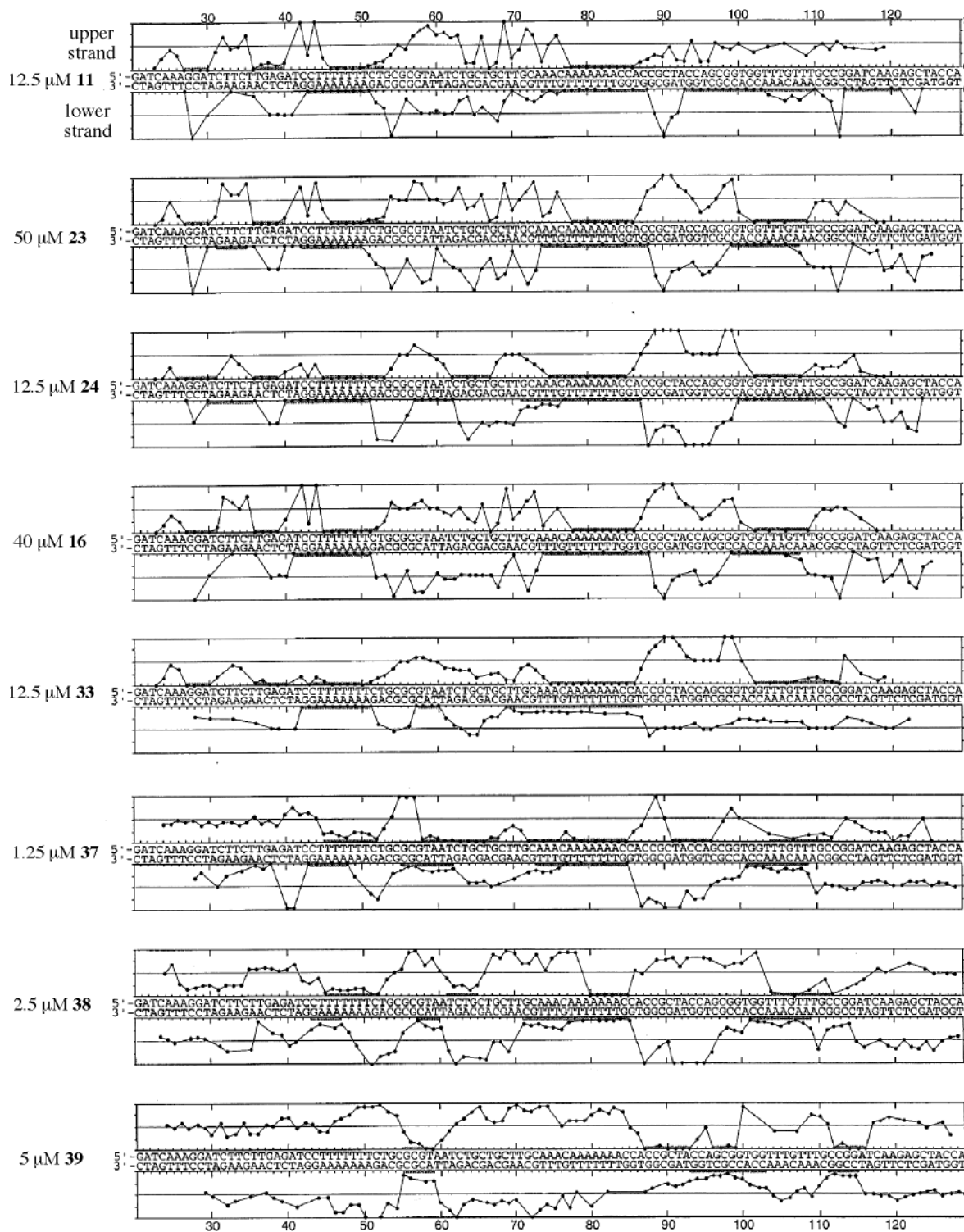


**Figure 11.** Differential DNase I cleavage plots in the presence of binders **11** (12.5  $\mu\text{M}$ ), **23** (50  $\mu\text{M}$ ), **24** (12.5  $\mu\text{M}$ ), **16** (40  $\mu\text{M}$ ), **33** (12.5  $\mu\text{M}$ ), **37** (1.25  $\mu\text{M}$ ), **38** (2.5  $\mu\text{M}$ ), and **39** (5.0  $\mu\text{M}$ ). The vertical scale corresponds to the ratio  $D/D_0$ , where  $D$  is the density of the band in the presence of a binder and  $D_0$  in its absence.

homopolymeric AT regions and overlap with those by distamycin A **37** and DAPI **38** (see, positions at  $\sim 50$  and  $\sim 80$  in the upper strand) but not with those by echinomycin **39** (Figures 10 and 11).<sup>47</sup> Such protection was not observed with  $\text{Zn}^{2+}$ –cyclen **2** (up to 100  $\mu\text{M}$ ), implying that the lipophilic aromatic pendants were essential for the  $\text{Zn}^{2+}$ –cyclen moiety to penetrate into the hydrophobic minor groove and interact with the poly AT regions in the native DNA. By contrast, the reversible interaction of the  $\text{Zn}^{2+}$ –cyclen

complexes with the GC-rich regions would not be strong enough to hinder the DNase I attack, although the acridine derivative **11** (e.g., 93–103 on the lower strand) and bisquinoline derivative **24** (e.g., 62–67 on the upper strand) seemed to have some minor interaction with the GC regions. The  $\text{IC}_{50}$  values (= concentration required for 50% inhibition of the DNase I digestion at position 45–50d(TpTpTpTpTpTpT) in the upper strand) were in the range of 8–30  $\mu\text{M}$ , values that might not be as remarkable as those of

**Table 1. One-Half the Concentration Values ( $IC_{50}$ )<sup>a</sup> of  $Zn^{2+}$ -Cyclen Derivatives (**11**, **23**, **24**, **32**, and **33**) and Minor Groove Binders (**37** and **38**) Required To Inhibit DNase I Hydrolysis of d(TpTpTpTpTpTpT) (45–50) in the Upper Strand<sup>47</sup>**

	$IC_{50}$ ( $\mu M$ )		$IC_{50}$ ( $\mu M$ )	
<b>11</b>	8	<b>33</b>	8	
<b>23</b>	30	<b>37</b>	0.5	
<b>24</b>	9	<b>38</b>	2	
<b>32</b>	25			

<sup>a</sup> The estimated error of the  $IC_{50}$  values was  $\pm 10\%$ .

0.5  $\mu M$  for **37** and 2  $\mu M$  for **38** (Table 1).<sup>47</sup> In the absence of  $Zn^{2+}$ , these ligands could not protect the AT-rich regions, meaning that  $Zn^{2+}$  is essential for interaction with DNA. The  $Cu^{2+}$  or  $Ni^{2+}$  complexes of acridinylmethylcyclen were not effective at all.

Next, to obtain a more microscopic picture of AT protection by the  $Zn^{2+}$ -cyclen derivatives, another DNA footprinting was conducted with another nuclease, micrococcal nuclease, a smaller enzyme (MW 16 800) that cuts DNA more effectively at the pA and

pT bonds rather than at the pG and pC bonds.<sup>54</sup> Moreover, micrococcal nuclease specifically works on a single-stranded sites in the breathing DNA without too much interference from the opposing strand. Thus, this enzyme should be useful in comparing similar AT recognition mode by the  $Zn^{2+}$ -cyclen derivatives and by distamycin A **37**. As expected, micrococcal nuclease footprinting (Figure 12) disclosed a more detailed picture about the interaction of the  $Zn^{2+}$ -cyclen complexes with the AT sites than did the DNase I footprinting described above.<sup>47</sup> Evidently, the  $Zn^{2+}$ -cyclen derivatives protected the pT bonds from micrococcal nuclease hydrolysis. Very interestingly, however, the  $Zn^{2+}$ -cyclen complexes did not protect the pairing pA at all. Note the well-hydrolyzed poly(dA) region near sequence number 80 in the upper strand and the well-protected (unhydrolyzed) corresponding partners of the poly(dT) region near 80 in the lower strand. The  $Zn^{2+}$  complexes rather served to promote the nuclease hydrolysis of homopolymeric dA regions, as illustrated by the denser footprint at the poly dA region.

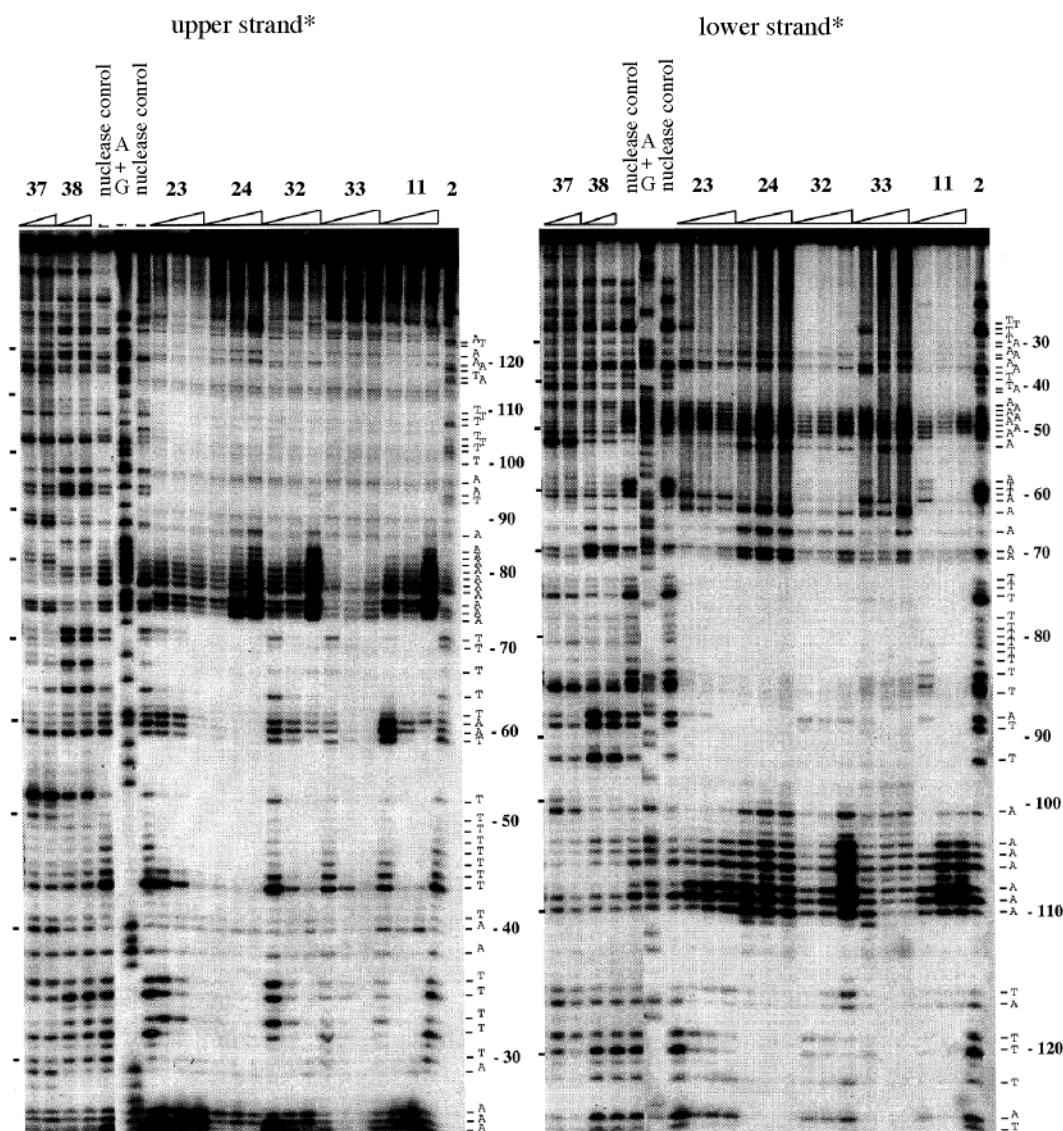
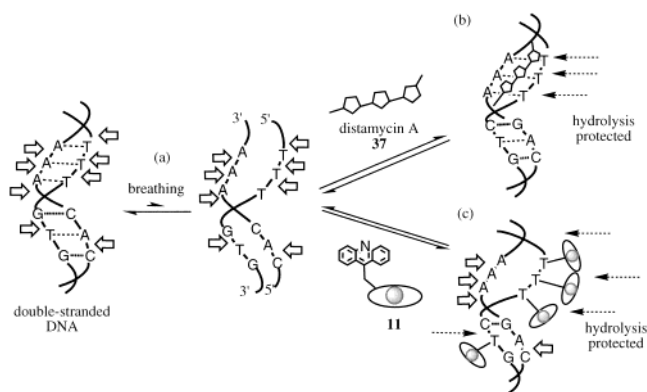


**Figure 12.** Micrococcal nuclease footprinting in the presence of **37** (5 and 10  $\mu M$ ), **38** (5 and 10  $\mu M$ ), **23** (40, 60, and 80  $\mu M$ ), **24** (10, 20, and 30  $\mu M$ ), **32** (20, 40, and 60  $\mu M$ ), **33** (5, 10, and 15  $\mu M$ ), **11** (10, 20, and 30  $\mu M$ ), and **2** (100  $\mu M$ ). The lane "nuclease control" represents DNA digested with DNase I without binders.

## Scheme 11



These results are summarized in Scheme 11, which shows that Zn<sup>2+</sup>-acridinylmethylcyclen **11** bound only to the thymine groups to disintegrate the A–T base pairs and that the separated A (adenine) partners were more exposed to micrococcal nuclease and more susceptible to the digestion by it. The arrows and dashed arrows in Scheme 11 indicate successful and failed hydrolysis by micrococcal nuclease, respectively. In the DNase I digestion (Figure 11), both paring partners T and A in the AT-rich regions were protected by the Zn<sup>2+</sup>-cyclen complexes.<sup>47</sup> DNase I tends to work on the double-stranded structure rather than the breathing single-stranded structure because DNase I, with its much larger size (MW 31 000),<sup>51c</sup> binds across the double strands at the minor groove. The exclusive binding of the Zn<sup>2+</sup>-cyclen derivatives to T in the A–T pairs was not shown by the first DNase I footprinting. With distamycin A **37** and DAPI **38**, the footprinting of micrococcal nuclease (Figure 12) clearly showed that both the pT and pA partners in the homopolymeric AT regions were well protected from the hydrolysis. This result implies that the minor groove binders **37** and **38** in an entirely opposite mechanism bind to both A and T in the AT minor groove to stabilize the double helix, as depicted in Scheme 11b. It was also found that **37** and the Zn<sup>2+</sup>-(4-quinolyl)methylcyclen complex **14** reversibly competed at the common AT regions.<sup>50</sup>

### 11. Selective Interaction with TATA Box and Inhibition of TATA Binding Protein to TATA Box by Zn<sup>2+</sup>-Cyclen Complexes

The AT-rich DNA sequence located at 25–30 base (“TATA box”) upstream from the transcriptional start sites is an essential element of the promoter for eukaryotic RNA polymerase II (Figure 13a).<sup>55</sup> The “TATA box” plays a key role in regulating the overall level of transcription and participates in selection of the transcriptional start sites. Some transcriptional factors (e.g., TATA binding protein and TBP) must bind to it for initiation of the transcription.<sup>56</sup> Distamycin A **37** and DAPI **38** were shown to strongly bind to the “TATA box” and thus inhibit the binding of TBP.<sup>57</sup>

A DNase I footprinting experiment on a 230 bp of SV40 early promoter fragment containing the TATA box showed that the Zn<sup>2+</sup>-cyclen derivatives, espe-

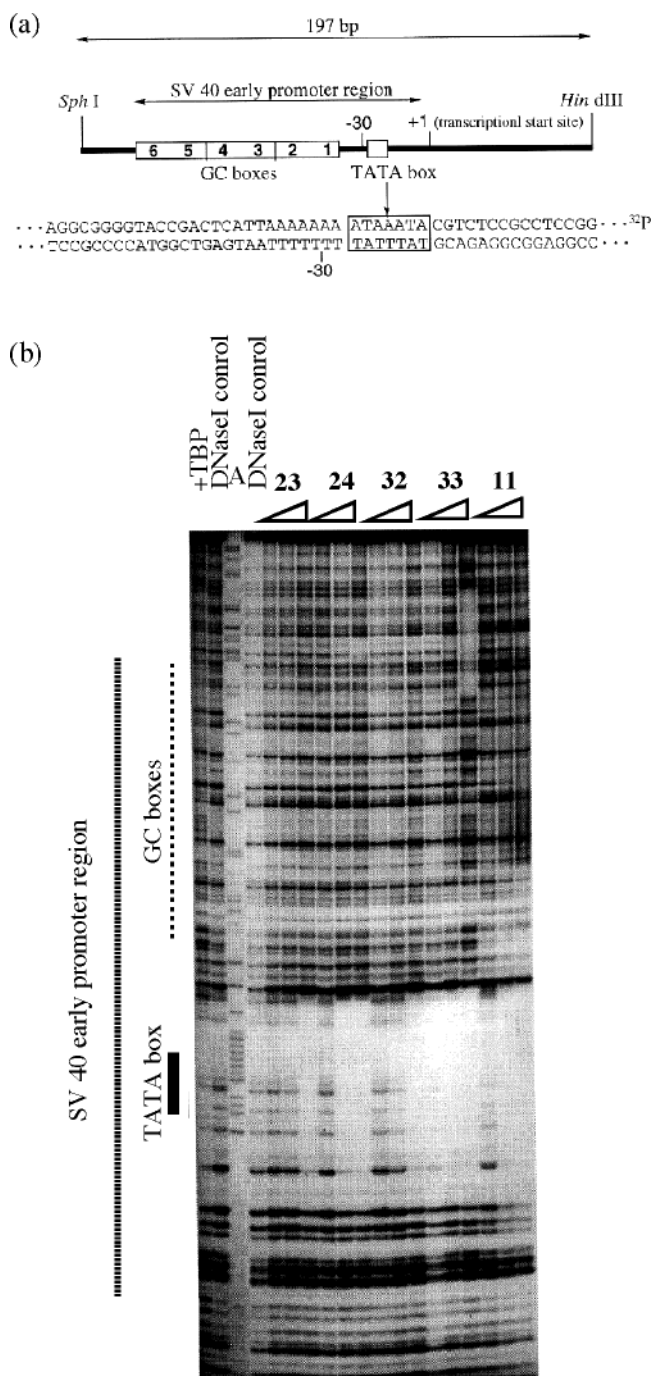


**Figure 13.** (a) Schematic representation of the SV40 early gene promoter region DNA (230 bp), with the DNA sequence of the TATA box region shown. (b) DNase I footprinting of 230-bp SV40 early gene promoter DNA in the presence of **23** (25, 50, and 100  $\mu$ M), **24** (3.13, 6.25, and 12.5  $\mu$ M), **32** (25, 50, and 100  $\mu$ M), **33** (1.56, 3.13, and 6.25  $\mu$ M), and **11** (6.25, 12.5, and 25  $\mu$ M). The lane labeled “A” represents the dideoxy sequencing marker specific for adenine. The lanes labeled “DNase I control” and “TBP” represent DNA digested with DNase I without binders and with TBP, respectively.

cially **11** and **33**, indeed bind selectively to the TATA box region (Figure 13b).<sup>48</sup> The inhibitory effect of those Zn<sup>2+</sup>-cyclen derivatives on the binding of human TBP to the TATA box was investigated by a gel mobility shift assay using a 25-bp TATA consensus DNA fragment (5′-GCAGAGCATATAAAAAT-GAGGTAGG-3′). Gel mobility shift assays of TBP in

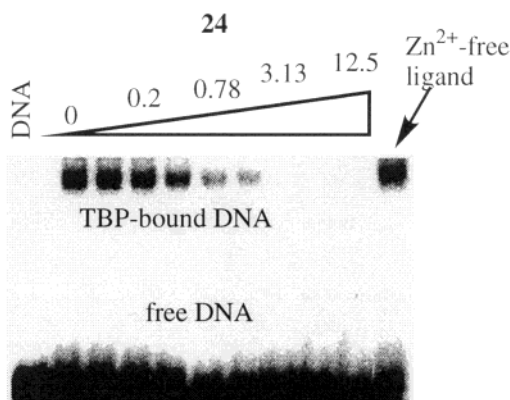


**Figure 14.** Gel mobility shift assay for a TATA box consensus DNA fragment in the presence of TBP, showing the titration with increasing amounts of **24** (0–50  $\mu\text{M}$ ). The lane labeled “DNA” represents DNA without TBP.

the absence and presence of **24** were performed. An increase in the concentration of the  $\text{Zn}^{2+}$ -cyclen derivatives reduced the concentration of the TBP–DNA complex (Figure 14). Conversely, the  $\text{Zn}^{2+}$ -free ligands showed no inhibitory effects on the TBP binding to DNA. These facts proved that formation of the TBP–TATA box complex was indeed inhibited by those  $\text{Zn}^{2+}$ -cyclen derivatives. The concentrations required for 50% inhibition ( $\text{IC}_{50}$ ) of the TBP–DNA complex formation were 15  $\mu\text{M}$  (for **11**), 70  $\mu\text{M}$  (for **23**), 2.5  $\mu\text{M}$  (for **24**), and 4  $\mu\text{M}$  (for **33**), which are not as remarkable as those for **37** (0.4  $\mu\text{M}$ ) and **38** (0.8  $\mu\text{M}$ ). However, this new biochemical reaction suggests that  $\text{Zn}^{2+}$ -cyclen derivatives may be a new useful prototype as a small molecular genetic transcriptional regulation factor.

Strangely, with the  $\text{Zn}^{2+}$ -anthraquinonylmethylcyclen complex **14**, selective recognition of consecutive G sequence was concluded from the DNase I footprinting of SV40 early promoter DNA fraction (197 bp) containing a TATA box and six GC boxes. It was found that **14** inhibited the Sp1 transcriptional factor protein from interacting with a GC box-consensus DNA.<sup>48</sup>

## 12. Inhibition of *in Vitro* dT-rich DNA-Directed Transcription by $\text{Zn}^{2+}$ -Cyclen Complexes

To test if the aforementioned chemical interaction of the  $\text{Zn}^{2+}$ -cyclen complexes with AT-rich region of

DNA affects subsequent biochemical processes,  $\text{Zn}^{2+}$ -cyclen complexes **2**, **11**, **24**, **32**, and **33** and their  $\text{Zn}^{2+}$ -free ligands were examined for their ability to inhibit *in vitro* transcription from calf thymus DNA as a template. The calf thymus DNA-directed transcription was assayed by measuring the incorporation of hot [ $^3\text{H}$ ]-UTP into the transcribed RNA in the presence of *E. coli* RNA polymerase. The reactants contained all other nucleotide substrates required for the RNA synthesis. The results showed that the transcription was inhibited by  $\text{Zn}^{2+}$ -cyclen complexes **11**, **24**, and **33**. Neither their free ligands nor free  $\text{Zn}^{2+}$  ions inhibited the incorporation of [ $^3\text{H}$ ]-UTP into RNA. The 50% inhibition concentrations ( $\text{IC}_{50}$ ) of the  $\text{Zn}^{2+}$ -cyclen complexes are summarized in Table 2.<sup>49</sup>

The inhibition profiles of  $\text{Zn}^{2+}$ -acridinylmethylcyclen **11** on the transcription of synthetic DNAs, i.e., poly(dA-dT)<sub>2</sub>, poly(dA)·poly(dT), and poly(dG-dC)<sub>2</sub> are shown in Figure 15.<sup>49</sup> For the poly(dA-dT)<sub>2</sub> template, incorporation of either [ $^3\text{H}$ ]-ATP or [ $^3\text{H}$ ]-UTP was inhibited to the same degree with  $\text{IC}_{50} = 36$  and 33  $\mu\text{M}$ , respectively. In contrast, for the poly(dA)·poly(dT) template the incorporation of [ $^3\text{H}$ ]-ATP ( $\text{IC}_{50} = 22$   $\mu\text{M}$ ) was not the same as that of [ $^3\text{H}$ ]-UTP ( $\text{IC}_{50} = 45$   $\mu\text{M}$ ), the former being more effectively blocked (Figure 15b). This fact matches the prediction that **11** strongly binds to the poly(dT) strand, so that the RNA polymerase would find difficulty in transcription with [ $^3\text{H}$ ]-ATP. Conversely, the transcription of the poly(dA) strand with [ $^3\text{H}$ ]-UTP would be little affected. For the poly(dG-dC)<sub>2</sub> template, the incorporation of [ $\alpha$ - $^{32}\text{P}$ ]-CTP was slightly inhibited ( $\text{IC}_{50} = 110$   $\mu\text{M}$ ), implying that the transcription of dG in this template was not as effectively blocked by **11** as that of dT in the AT polymers (Figure 15c).

Inhibition of the incorporation of [ $^3\text{H}$ ]-ATP and [ $^3\text{H}$ ]-UTP into RNA by *p*-bis( $\text{Zn}^{2+}$ -cyclen) **16** and a linear tris( $\text{Zn}^{2+}$ -cyclen) **18** was also examined (Figure 16 and Table 2).<sup>58</sup> When calf thymus DNA was used as a template, the trimeric **18** exhibited the most potent inhibitory effect ( $\text{IC}_{50} = 60$   $\mu\text{M}$ ), while this value is larger than  $\text{IC}_{50}$  (8–9  $\mu\text{M}$ ) of distamycin A **37**. In contrast, when poly(dA-dT)<sub>2</sub> was used as a template,  $\text{IC}_{50}$  of **18** (1.2  $\mu\text{M}$  for [ $^3\text{H}$ ]-ATP uptake and 1  $\mu\text{M}$  for [ $^3\text{H}$ ]-UTP uptake) became as low as those for distamycin A **37** (1.4  $\mu\text{M}$  for [ $^3\text{H}$ ]-ATP uptake and 1.6  $\mu\text{M}$  for [ $^3\text{H}$ ]-UTP uptake). The most illustrative

**Table 2.** One-Half the Concentration Value ( $\text{IC}_{50}$ ) of  $\text{Zn}^{2+}$ -Cyclen Derivatives (**2**, **11**, **23**, **24**, **32**, **33**, **16**, and **18**) and Distamycin A (**37**) To Inhibit Poly(dA)·poly(dT)-directed Transcription of DNA (Calf Thymus DNA, Poly(dA-dT)<sub>2</sub>, and Poly(dA)·poly(dT))<sup>49,58</sup>

template complex	$\text{IC}_{50}$ ( $\mu\text{M}$ )					
	calf thymus DNA		poly(dA-dT) <sub>2</sub>		poly(dA)·poly(dT)	
	[ $^3\text{H}$ ]-UTP	[ $^3\text{H}$ ]-ATP	[ $^3\text{H}$ ]-UTP	[ $^3\text{H}$ ]-ATP	[ $^3\text{H}$ ]-UTP	[ $^3\text{H}$ ]-ATP
<b>2</b>	>300	>300	>100	>100	>100	>100
<b>11</b>	130	150	33	36	45	22
<b>23</b>	>200	>200	n.d. <sup>a</sup>	n.d. <sup>a</sup>	n.d. <sup>a</sup>	n.d. <sup>a</sup>
<b>24</b>	95	>200	n.d. <sup>a</sup>	n.d. <sup>a</sup>	n.d. <sup>a</sup>	n.d. <sup>a</sup>
<b>32</b>	>200	>200	n.d. <sup>a</sup>	n.d. <sup>a</sup>	n.d. <sup>a</sup>	n.d. <sup>a</sup>
<b>33</b>	55	>200	n.d. <sup>a</sup>	n.d. <sup>a</sup>	n.d. <sup>a</sup>	n.d. <sup>a</sup>
<b>16</b>	300	300	50	60	60	40
<b>18</b>	60	60	1	1.2	40	0.8
<b>37</b>	9	8	1.6	1.4	1.0	0.8

<sup>a</sup> n.d.: not determined.

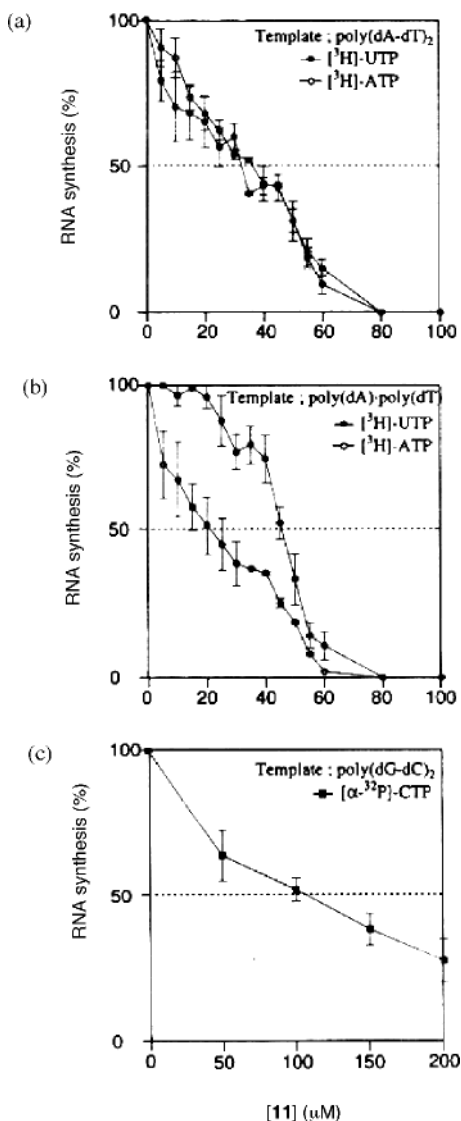


**Figure 15.** Inhibition profiles of in vitro transcription by **11** (a)  $[^3\text{H}]$ -ATP and  $[^3\text{H}]$ -UTP incorporation directed by the poly(dA-dT)<sub>2</sub> template, (b)  $[^3\text{H}]$ -ATP and  $[^3\text{H}]$ -UTP incorporation directed by the poly(dA)·poly(dT) template, and (c)  $[\alpha\text{-}^{32}\text{P}]$ -CTP incorporation directed by the poly(dG-dC)<sub>2</sub> template.

inhibitory effect by **18** was observed when poly(dA)·poly(dT) was used as a template. The IC<sub>50</sub> value of **18** for  $[^3\text{H}]$ -ATP incorporation was 0.8  $\mu\text{M}$ . In sharp contrast, IC<sub>50</sub> of **18** for  $[^3\text{H}]$ -UTP incorporation was 40  $\mu\text{M}$ , indicating that tris(Zn<sup>2+</sup>-cyclen) **18** selectively inhibits transcription from the poly(dT) strand but not from the poly(dA) in the double-stranded poly(dA)·poly(dT).<sup>58</sup>

### 13. Lipophilic Zn<sup>2+</sup>-Cyclen Complexes as Effective Carriers of AZT

A variety of nucleoside drugs such as AZT, 2',3'-dideoxycytidine (ddC), and 2',3'-dideoxyadenosine (ddA) are currently used in the treatment of AIDS.<sup>59</sup> These drugs enter cells primarily by simple passive diffusion<sup>60</sup> and then undergo phosphorylation to each ultimate nucleotide triphosphate derivative to act against HIV reverse transcriptase.<sup>61</sup> Therefore, the development of lipophilic carriers for these nucleotide

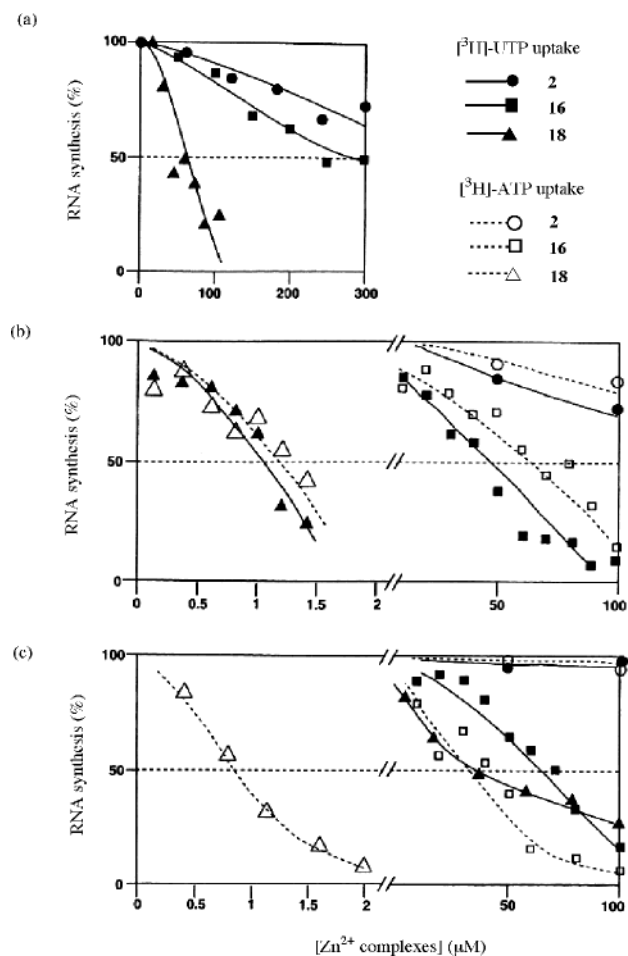


**Figure 16.** Inhibition profiles of DNA-directed in vitro RNA synthesis by **2**, **16**, and **18** (a)  $[^3\text{H}]$ -UTP incorporation directed by calf thymus DNA, (b)  $[^3\text{H}]$ -ATP or  $[^3\text{H}]$ -UTP incorporation directed by the poly(dA-dT)<sub>2</sub> template, and (c)  $[^3\text{H}]$ -ATP or  $[^3\text{H}]$ -UTP incorporation directed by the poly(dA)·poly(dT) template.

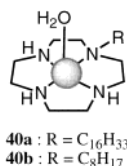
phosphates might be of great help in increasing the efficacy of the drugs. So far, no selective carriers or delivery system for dT or U nucleotides are known. If available, they would be extremely useful, for instance, in the effective administration of AZT.

Lipophilic Zn<sup>2+</sup>-cyclen derivatives such as Zn<sup>2+</sup>-hexadecylcyclen complex **40a** were synthesized for selective and effective carriers of dT and U.<sup>62</sup> For example, dT and U (1 mM), which were negligibly transferred into organic layer without carriers, were successfully extracted from an aqueous phase at pH 9.0 (50 mM HEPES with *I* = 0.1 (NaNO<sub>3</sub>)) into the CHCl<sub>3</sub> phase by an equimolar **40a** in 22% and 13% yield, respectively, while other nucleosides (A, G, and C) were not extracted. Interestingly, more lipophilic AZT was extracted into the CHCl<sub>3</sub> layer from an aqueous solution in 91% at pH 7.6, while AZT extraction in the absence of **40a** was only 17% under the same conditions. The log *K*<sub>s</sub> values for the interaction of Zn<sup>2+</sup>-octylcyclen **40b** with dT and AZT in aqueous solution at pH 7.6 and 25 °C were 3.2 and 3.4, respectively, implying that 47% and 53% complexation occurred at [total **40b**] = [total dT (or AZT)] = 1 mM in aqueous solution. Using a U-shaped liquid membrane system, we observed the migration of dT and AZT by **40a** from aqueous phase I (pH 9) to

**Table 3.** Extraction of Nucleosides and Nucleotides by CHCl<sub>3</sub> Solution Containing Zinc(II)–Cyclen Carriers at 25 °C<sup>62</sup>

nucleoside or nucleotide	carrier	pH of aqueous layer	extraction efficiency (%)
dT	none	9.0	<1
dT	<b>40a</b>	9.0	22 ± 2
dT	<b>40a</b>	7.6	8 ± 1
dT	<b>40b</b>	9.0	12 ± 1
U	none	9.0	<1
U	<b>40a</b>	9.0	13 ± 1
dC	<b>40a</b>	9.0	<1
dA	<b>40a</b>	9.0	<1
dG	<b>40a</b>	9.0	<2
AZT	none	7.6	17 ± 1
AZT	<b>40a</b>	7.6	91 ± 1
1-MeT	none	7.6	25 ± 1
1-MeT	<b>40a</b>	7.6	91 ± 1
Ff	none	7.6	41 ± 1
Ff	<b>40a</b>	7.6	>98
5'-dTMP	none	9.0	<1
5'-dTMP	<b>40a</b>	9.0	18 ± 1
AZTMP	none	7.6	<1
AZTMP	<b>40a</b>	7.6	37 ± 1

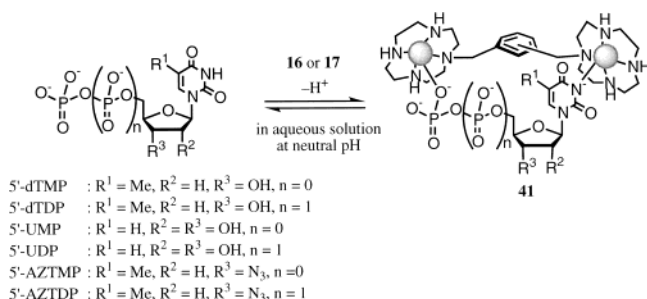
aqueous phase II (pH 5) through a CHCl<sub>3</sub> layer. The dT nucleotides such as 5'-dTMP, 5'-dTTP, and AZTMP were also extracted from a pH 7.6 aqueous solution into organic solution in moderate yields (Table 3).<sup>62</sup>



#### 14. Selective and Efficient Recognition of Thymidine Mono- (dTMP) and Diphosphate (dTDP) Nucleotides by the Ditopic Receptors Bis(Zn<sup>2+</sup>–cyclen) Complexes

Up to this stage, it was recognized that Zn<sup>2+</sup>–cyclen **2** interacted with phosphate dianions as well as thymine.<sup>11–15,63</sup> Thus, it was postulated that the *p*-bis(Zn<sup>2+</sup>–cyclen) **16** and *m*-bis(Zn<sup>2+</sup>–cyclen) **17** could be good ditopic receptors for phosphates of dT (or U) nucleosides (thymidine mononucleotide (3'- and 5'-dTMP) or uridine mononucleotide (3'- and 5'-UMP)) (Scheme 12).<sup>64,65</sup> The complexation constant,

##### Scheme 12



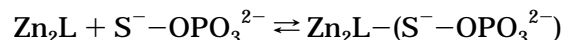
log *K<sub>s</sub>* for the bis(Zn<sup>2+</sup>–cyclen)-5'-dTMP complex **41** defined by eq 5 (*S*<sup>-</sup> is the deprotonated thymine part) at 25 °C with *I* = 0.10 (NaNO<sub>3</sub>) was determined to be 9.6 by the potentiometric pH, from which an

**Table 4.** Apparent Complexation Constants (log *K<sub>app</sub>*) for Imide-Containing Nucleotides with Zinc(II)–Cyclen Complexes at pH 7.6 and 25 °C Determined by Potentiometric pH Titration,<sup>a</sup> Isothermal Titration Calorimetry (in 50 mM HEPES buffer),<sup>b</sup> and UV Titration (in 50 mM HEPES buffer)<sup>c</sup> with *I* = 0.1 (NaNO<sub>3</sub>)<sup>64</sup>

	<b>13</b>	<b>17</b>	<b>16</b>
dT	3.2 <sup>a</sup> (5.7) <sup>d</sup>		3.2, 3.2 <sup>b</sup> ( <b>16</b> :dT = 1:2)
3'-dTMP		5.2 <sup>a</sup> (8.6) <sup>c</sup> 5.3 <sup>b</sup> 5.4 <sup>c,f</sup>	5.9 <sup>a</sup> (8.9) <sup>d</sup> 5.8 <sup>b</sup> 5.8 <sup>c</sup>
5'-dTMP	3.4, 3.4 <sup>b</sup> ( <b>13</b> :5'-dTMP = 2:1)	5.5 <sup>a</sup> (9.3) <sup>d</sup> 5.5 <sup>b</sup> 5.7 <sup>c</sup>	6.4 <sup>a</sup> (9.6) <sup>d</sup> >6 <sup>b</sup> >6 <sup>c</sup>
3'-UMP		4.8 <sup>a</sup> (7.8) <sup>c</sup> 5.2 <sup>c</sup>	5.5 <sup>a</sup> (8.5) <sup>d</sup> 5.7 <sup>c</sup>
5'-UMP		5.4 <sup>a</sup> (8.3) <sup>d</sup> 5.5 <sup>b</sup>	6.2 <sup>a</sup> (8.8) <sup>d</sup> >6 <sup>b</sup> >6 <sup>c</sup>
5'-dTDP		5.6 <sup>b</sup> 5.5 <sup>c</sup>	>6 <sup>b</sup> >6 <sup>c</sup>
5'-dTTP		5.0 <sup>b</sup>	5.6 <sup>c</sup>
5'-AZTMP		5.5 <sup>b</sup> 5.7 <sup>c</sup>	>6 <sup>b</sup> >6 <sup>c</sup>
5'-AZTDP		5.3 <sup>b</sup> 5.5 <sup>c</sup>	5.9 <sup>b</sup> >6 <sup>c</sup>

<sup>a–c</sup> See the text for the definition of *K<sub>app</sub>* and experimental conditions. The experimental errors were ±3%. <sup>d</sup> Intrinsic complexation constants *K<sub>s</sub>*.

apparent complex formation constant, log *K<sub>app</sub>* (defined by eqs 6–8), at pH 7.6 was calculated to be 6.4 (i.e., *K<sub>d</sub>* ~ μM order). A speciation diagram for 5'-dTMP (1 mM) and **16** (1 mM) as a function of pH at 25 °C with *I* = 0.1 (NaNO<sub>3</sub>) shows that the population of the 1:1 complex (**41**) is greater than 95% at 6.6 < pH < 8.8.<sup>64</sup>



$$K_s = \frac{[(\text{Zn}_2\text{L}) - (\text{S}^- - \text{OPO}_3^{2-})]}{[\text{Zn}_2\text{L}(\text{OH}_2)_2][\text{S}^- - \text{OPO}_3^{2-}](\text{M}^{-1})} \quad (5)$$

$$K_{\text{app}} = \frac{[(\text{Zn}_2\text{L}) - (\text{S}^- - \text{OPO}_3^{2-})]}{[\text{Zn}_2\text{L}]_{\text{free}}[\text{S}^- - \text{OPO}_3^{2-}]_{\text{free}}(\text{at designated pH})(\text{M}^{-1})} \quad (6)$$

$$[\text{Zn}_2\text{L}]_{\text{free}} = [\text{Zn}_2\text{L}(\text{OH}_2)_2] + [\text{Zn}_2\text{L}(\text{OH}_2)(\text{OH}^-)] + [\text{Zn}_2\text{L}(\text{OH}^-)_2] \quad (7)$$

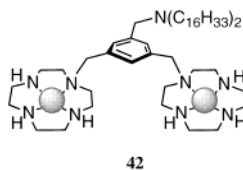
$$[\text{S}^- - \text{OPO}_3^{2-}]_{\text{free}} = [\text{S}^- - \text{OPO}_3\text{H}_2] + [\text{S}^- - \text{OPO}_3\text{H}^-] + [\text{S}^- - \text{OPO}_3^{2-}] \quad (8)$$

The complexation constants, *K<sub>app</sub>*, of **16** and **17** with various nucleotides are summarized in Table 4. The complexation of those dT nucleotides with the ditopic receptors (log *K<sub>app</sub>* values in the range of more than 5.6 with **16** and 5.0–6.4 with **17**) is ca. 40–1000 times more favorable than with the monotopic **13** (log *K<sub>app</sub>* = 3.4), due to the additive binding effect of the dibasic phosphate to the second Zn<sup>2+</sup>–cyclen moieties in **16** and **17**. That the *p*-bis(Zn<sup>2+</sup>–cyclen) **16** was generally a better receptor than the *m*-isomer **17**



might be due to the more appropriate distance between two  $\text{Zn}^{2+}$ s for better interaction. On the  $^1\text{H}$  NMR (500 MHz) spectra of the 5'-dTMP complex (1 mM) with **16** in  $\text{D}_2\text{O}$  at  $\text{pD } 7.8 \pm 0.1$  and  $35^\circ$ , two independent sets of peaks appeared, indicating that (1) the quantitative 1:1 complexation of 5'-dTMP with **16** occurred and (2) the 1:1 complex was kinetically inert on the NMR time scale (500 MHz).

The phosphorylation of AZTMP to AZTDP catalyzed by thymidylate kinase (ATP:dTMP phosphotransferase) is rate determining in the metabolic pathway of AZT,<sup>66</sup> and some kinase-deficient cells such as macrophages become reservoirs for HIV.<sup>67</sup> Therefore, the most effective form of administration may be AZTDP or AZTTP rather than AZT. However, cell permeation with the former nucleotides is difficult due to their highly ionic characteristics. Appropriate attachment of lipophilic functions to **16** or **17** might make novel AZT administration agents for dT-nucleotide drugs. Consequently, a bis( $\text{Zn}^{2+}$ -cyclen) having an alkyl long chain **42** was designed. Unfortunately, extraction of dT nucleotides such as 5'-dTMP and 5'-AZTMP by **42** was not as conclusive because of micelle formation. However, isothermal calorimetric titrations of **42** with 5'-dTMP and 5'-AZTMP in a micelle solution at pH 7.4 (50 mM HEPES with  $I = 0.1$  ( $\text{NaNO}_3$ )) containing 10 mM Triton X-100 gave dissociation constants,  $K_d$ , for **42**–5'-dTDP (13  $\mu\text{M}$ ) and **42**–AZTDP (8  $\mu\text{M}$ ) complexes which are close to the  $K_d$  values for **16**–5'-dTMP (4.0  $\mu\text{M}$ ) and **16**–AZTDP (10  $\mu\text{M}$ ) complexes determined under the same conditions.<sup>68</sup> These derivatives also would be useful in the separation and detection of various imide-containing nucleotides.



Moreover, **16** and **17** and their free ligands had already been discovered to possess extremely potent anti-HIV activity.<sup>69–71</sup> It was proposed that bis-(macrocylic tetraamine)s act as specific inhibitors of the interaction between HIV gp120 and a coreceptor of T cell (chemokine receptors such as CXCR4), thereby blocking the invasion of T cells by HIV.<sup>70</sup> It will be interesting to see if the combination of the two mechanistically different kinds of anti-HIV active agents, AZT nucleotides and the bis( $\text{Zn}^{2+}$ -cyclen) derivatives, may offer a new cocktail for AIDS treatment.

### 15. Potent Inhibition of HIV-1 TAR RNA-Tat Peptide Binding by $\text{Zn}^{2+}$ Complexes

Some promising methodologies for AIDS therapy are to prevent the formation of complexes of key viral RNA with proteins or to cleave specific RNA sites.<sup>72</sup> Transcription of the HIV-1 genome is facilitated by a HIV-1 regulatory protein, Tat, which activates the synthesis of full-length HIV-1 mRNA by binding to a TAR (*trans*-activation responsive) element RNA.<sup>73</sup>

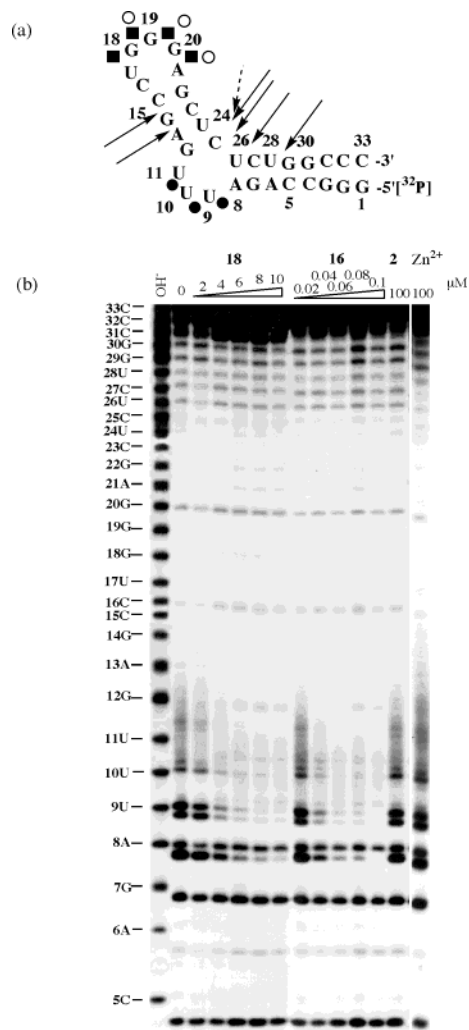


**Figure 17.** (a) TAR model ( $\text{TAR}_{33}$ ) containing residues 17–43 of HIV-1 mRNA and three additional GC pairs. The sequence is shown with a schematic summary of the protection sites by **18** from micrococcal nuclease (black circles), RNase A (black squares), and phosphodiesterase I (open circles). Enhanced cleavage sites by RNase A (dashed arrow) and phosphodiesterase I (arrow) are shown. (b) Micrococcal nuclease footprinting of  $\text{TAR}_{33}$  in the presence of **18**, **16**, **2**, or  $\text{ZnSO}_4$ . The concentrations of the compounds are shown above each lane. The lane labeled “OH<sup>-</sup>” represents the alkaline hydrolysis marker.

A direct correlation has been found between the binding of Tat to TAR RNA and up-regulation of HIV-1 mRNA transcription.<sup>74</sup> The TAR element consisting of the first 59 nucleotides of the HIV-1 primary transcript adopts a hairpin structure with a U-rich bulge (UUU or UCU) located four base pairs below a six-nucleotide loop. The UUU bulge is the Tat binding site, and the loop is a homing site for cellular proteins.<sup>75</sup> Aminoglycoside antibiotics (e.g., neomycin) currently seem to have the highest affinity to the bulge part, showing the most potent inhibition ( $\text{IC}_{50} = 1 \mu\text{M}$ ) of the formation of the TAR RNA-Tat protein complex.

Footprinting analysis using micrococcal nuclease has revealed the UUU bulge to be strongly protected by *p*-bis( $\text{Zn}^{2+}$ -cyclen) **16** and tris( $\text{Zn}^{2+}$ -cyclen) **18** in the TAR model sequence ( $\text{TAR}_{33}$ , for its sequence, see Figure 17a).<sup>76</sup> The sequence ladder without  $\text{Zn}^{2+}$  complex shows that the 5'-phosphates of A6, A8, U9,

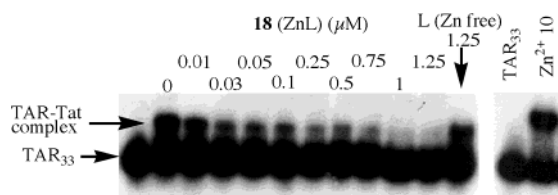


**Figure 18.** Gel mobility shift of the complex of TAR<sub>33</sub> and Tat<sub>46–86</sub> (9.1 nM) in the presence of increasing concentrations of **18** (0–1.25 μM) or ZnSO<sub>4</sub> (10 μM). The lane labeled “TAR<sub>33</sub>” indicates uncomplexed TAR<sub>33</sub>.

and U10 (Figure 17b) are cleaved to produce the 3'-phosphate and/or 2',3'-phosphate termini of 5C, 7G, 8A, and 9U, respectively. The protected sites of TAR<sub>33</sub> are indicated by the filled circles in Figure 17a. The 50% inhibition concentrations (IC<sub>50</sub>) of the 5'-phosphate hydrolysis of U10 were determined to be 3 μM for **16** and 25 nM for **18**, while it was >100 μM for **2**.

The inhibition of the TAR<sub>33</sub>–Tat consensus peptide (Tat<sub>47–86</sub>, YGRKKRRQRRRPRQGSQTHQVSLSKOPTSQRGDPTGPK) by tris(Zn<sup>2+</sup>–cyclen) **18** was examined by gel mobility shift assay (Figure 18).<sup>76</sup> The *K<sub>d</sub>* value for the TAR<sub>33</sub>–Tat complexation and the IC<sub>50</sub> value of **18** were determined to be 15 and 20 nM, respectively, showing that tris(Zn<sup>2+</sup>–cyclen) **18** may serve in a novel methodology for the treatment of AIDS.

## 16. Summary

On the basis of earlier biomimetic studies of the acidic and labile properties of zinc(II)-bound H<sub>2</sub>O in biological environments, a variety of derivatives of Zn<sup>2+</sup>–cyclen complexes have been designed as novel prototypes of selective receptors of “imide”-containing nucleobases, thymine (dT) and uracil (U), in aqueous solution at physiological pH. The Zn<sup>2+</sup>–cyclen complexes with polyaromatic pendants possess recognition efficiency in terms of *K<sub>d</sub>* on the order of 10 μM (for the 1:1 complexes with dT<sup>–</sup> or U<sup>–</sup>) in single- and double-stranded DNA (or RNA) so as to disrupt A–dT (or A–U) hydrogen bonds in double-stranded nucleic acids. These cyclen complexes bind to a biologically essential AT-rich element, TATA box, to inhibit a transcriptional factor TATA binding protein from binding to the TATA box. Bis(Zn<sup>2+</sup>–cyclen) complexes and a linear tris(Zn<sup>2+</sup>–cyclen) complex have been synthesized to sequence-selectively recognize a dinucleotide, d(TpT), and a trinucleotide, d(TpTpT), respectively. The *K<sub>d</sub>* values for these ternary complexes are on the orders of micromolar and nanomolar, respectively. These recognitions have been successfully applied to the effective inhibition of poly(dT)-template RNA synthesis and the inhibition of TAR RNA–Tat protein binding. Lipophilic derivatives of monomeric and dimeric Zn<sup>2+</sup>–cyclen complexes have been shown to be selective carriers for dT (or U) nucleosides and nucleotides, affording new prototype drug-delivery systems for some antiviral agents. In vitro anti-HIV and antimicrobial activities of the Zn<sup>2+</sup>–cyclen derivatives have also been revealed. Furthermore, the present principle of the interaction of multinuclear Zn<sup>2+</sup> complexes with nucleic acids has recently been extended to the

construction of novel three-dimensional supra-molecular cage complexes in aqueous solution.<sup>77</sup> In conclusion, basic studies of the intrinsic properties of Zn<sup>2+</sup> have led to a new area of biomimetic chemistry involving novel molecular recognition, pharmaceutical chemistry, and supramolecular chemistry.

## 17. References

- (1) Alberts, B.; Bray, D.; Lewis, J.; Raff, M.; Roberts, K.; Watson, J. D. *The Molecular Biology of the Cell*; Garland: New York, 1983; p 435.
- (2) Cech, T. R. *Science* **1987**, *236*, 1532.
- (3) McClellin, J. A.; Frederick, B. C.; Wang, B. C.; Greene, P.; Boyer, H. W.; Grable, J.; Rosenberg, J. M. *Science* **1986**, *234*, 1526.
- (4) (a) Kimura, E.; Kodama, M.; Yatsunami, T. *J. Am. Chem. Soc.* **1982**, *112*, 3182. (b) Kimura, E. *Top. Curr. Chem.* **1985**, *128*, 113. (c) Kimura, E. *Crown Ethers and Analogous Compounds*; Hiraoka, M., Ed.; Elsevier: Amsterdam, 1992; p 381.
- (5) Hosseini, M. W.; Blacker, A. J.; Lehn, J. M. *J. Am. Chem. Soc.* **1990**, *112*, 3896.
- (6) Feibush, B.; Figueroa, A.; Charles, R.; Onan, K. D.; Feibush, P.; Karger, B. L. *J. Am. Chem. Soc.* **1986**, *108*, 3310.
- (7) (a) Hamilton, A. D.; van Engen, D. *J. Am. Chem. Soc.* **1987**, *109*, 5035. (b) Chang, S. K.; Hamilton, A. D. *J. Am. Chem. Soc.* **1988**, *110*, 1318. (c) Chang, S. K.; Engen, D. V.; Fan, E.; Hamilton, A. D. *J. Am. Chem. Soc.* **1991**, *113*, 7640.
- (8) Conn, M.; Frederick, C. A.; Wang, A. H. J.; Rich, A. *Proc. Natl. Acad. Sci. U.S.A.* **1987**, *84*, 8385.
- (9) Kral, U.; Sesler, J.; Furuta, H. *J. Am. Chem. Soc.* **1992**, *114*, 8704.
- (10) (a) Lippert, B. *Cisplatin, Chemistry and Biochemistry of a Leading Anticancer Drug*; Wiley-VCH: New York, 1999. (b) Lippert, B. *Coord. Chem. Rev.* **1999**, *182*, 263.
- (11) (a) Kimura, E.; Shiota, T.; Koike, M.; Kodama, M. *J. Am. Chem. Soc.* **1990**, *112*, 5805. (b) Koike, T.; Kimura, E. *J. Am. Chem. Soc.* **1991**, *113*, 8935. (c) Zhang, X.; van Eldik, R.; Koike, T.; Kimura, E. *Inorg. Chem.* **1993**, *32*, 5749.
- (12) (a) Kimura, E. *Comm. Inorg. Chem.* **1991**, *11*, 285. (b) Kimura, E.; Shionoya, M. *Metal Ions in Biological Systems*; Sigel, A., Sigel, H. Eds.; Marcel Dekker: New York, 1996; Vol. 33, p 29. (c) Kimura, E.; Koike, T. In *Comprehensive Supramolecular Chemistry*; Reinhoudt, D. N., Ed.; Pregamon: Tokyo, 1996; Vol. 10, p 429. (d) Kimura, E.; Koike, T.; Shionoya, M. In *Structure and Bonding: Metal Site in Proteins and Models*; Sadler, J. P., Ed.; Springer: Berlin, 1997; Vol. 89, p 1. (e) Kimura, E. *Curr. Opin. Chem. Biol.* **2000**, *4*, 207. (f) Kimura, E.; Koike, T. In *Bioinorganic Catalysis*; Reedijk, J., Bouwman, E., Eds.; Marcel Dekker, Inc: New York, 1999; p 33. (g) Kimura, E. *Acc. Chem. Res.* **2001**, *34*, 171.
- (13) Koike, T.; Kimura, E.; Nakamura, I.; Hashimoto, Y.; Shiro, M. *J. Am. Chem. Soc.* **1992**, *114*, 7338.
- (14) (a) Koike, T.; Watanabe, T.; Aoki, S.; Kimura, E.; Shiro, M. *J. Am. Chem. Soc.* **1996**, *118*, 12696. (b) Kimura, E.; Aoki, S.; Kikuta, M.; Koike, T. *Proc. Natl. Acad. Sci. U.S.A.* **2003**, *100*, 3731. (c) Aoki, S.; Kaido, S.; Fujioka, H.; Kimura, E. *Inorg. Chem.* **2003**, *42*, 1023. (d) Koike, T.; Abe, T.; Takahashi, M.; Ohtani, K.; Kimura, E.; Shiro, M. *J. Chem. Soc., Dalton Trans.* **2002**, 1764.
- (15) (a) Kimura, E.; Koike, T. *Chem. Soc. Rev.* **1998**, *27*, 179. (b) Kimura, E. *S. Afr. J. Chem.* **1997**, *50*, 240. (c) Kimura, E.; Aoki, S. *BioMetals* **2001**, *14*, 191.
- (16) Kimura, E.; Koike, T. *J. Chem. Soc., Chem. Commun.* **1998**, 1495.
- (17) Drohat, A. C.; Jagadeesh, J.; Ferguson, E.; Stivers, J. T. *Biochemistry* **1999**, *38*, 11866.
- (18) Shionoya, M.; Kimura, E.; Shiro, M. *J. Am. Chem. Soc.* **1993**, *115*, 6730.
- (19) Shionoya, M.; Sugiyama, M.; Kimura, E. *J. Chem. Soc., Chem. Commun.* **1994**, 1747.
- (20) (a) Kimura, E.; Kikuta, E. *J. Biol. Inorg. Chem.* **2000**, *5*, 139. (b) Kimura, E.; Kikuta, E. *Prog. React. Kinet. Mech.* **2000**, *25*, 1.
- (21) Sigel, H. *Chem. Soc. Rev.* **1993**, *22*, 255.
- (22) Chen, H.; Parkinson, J. A.; Parson, S.; Coxall, R. A.; Gould, R. O.; Sadler, P. J. *J. Am. Chem. Soc.* **2002**, *124*, 3064.
- (23) Mancini, F.; Chin, J. *J. Am. Chem. Soc.* **2002**, *124*, 10946.
- (24) (a) Breslow, R.; Berger, D.; Huang, D.-L. *J. Am. Chem. Soc.* **1990**, *112*, 3686. (b) Chu, F.; Smith, J.; Lynch, V. M.; Anslyn, E. V. *Inorg. Chem.* **1995**, *34*, 5689. (c) Chapman, W. H., Jr.; Breslow, R. *J. Am. Chem. Soc.* **1995**, *117*, 5462. (d) Yashiro, M.; Ishikubo, A.; Komiyama, M. *J. Chem. Soc., Chem. Commun.* **1995**, 1793. (e) Yashiro, M.; Ishikubo, A.; Komiyama, M. *J. Chem. Soc., Chem. Commun.* **1997**, 83.
- (25) (a) Berg, J. M. *Annu. Rev. Biophys. Chem.* **1990**, *19*, 405. (b) Pavletch, N. P.; Pabo, C. C. *Science* **1991**, *252*, 809. (c) Coleman, J. E. *Annu. Rev. Biochem.* **1992**, *61*, 897. (d) Berg, J.

- M. *Acc. Chem. Res.* **1995**, *28*, 14. (e) Greisman, H. A.; Pabo, C. O. *Science* **1997**, *275*, 657.
- (26) Shionoya, M.; Ikeda, T.; Kimura, E.; Shiro, M. *J. Am. Chem. Soc.* **1994**, *116*, 3848.
- (27) Tucker, J. H. R.; Shionoya, M.; Koike, T.; Kimura, E. *Bull. Chem. Soc. Jpn.* **1995**, *68*, 2465.
- (28) Koike, T.; Gotoh, T.; Aoki, S.; Kimura, E.; Shiro, M. *Inorg. Chim. Acta* **1998**, *270*, 424.
- (29) Koike, T.; Takashige, M.; Kimura, E.; Fujioka, H.; Shiro, M. *Chem. Eur. J.* **1996**, *2*, 617.
- (30) Fujioka, H.; Koike, T.; Yamada, N.; Kimura, E. *Heterocycles* **1996**, *42*, 775.
- (31) Kimura, E.; Kikuchi, M.; Kitamura, H.; Koike, T. *Chem. Eur. J.* **1999**, *5*, 3113.
- (32) Kimura, E.; Kitamura, H.; Ohtani, K.; Koike, T. *J. Am. Chem. Soc.* **2000**, *122*, 4668.
- (33) Kimura, E.; Katsube, N.; Koike, T.; Shiro, M.; Aoki, S. *Supramol. Chem.* **2002**, *14*, 95.
- (34) (a) Friedberg, E.; Walker, G. C.; Siede, W. *DNA Repair and Mutagenesis*; ASM Press: Washington, D.C., 1995. (b) Taylor, J.-S. *Pure Appl. Chem.* **1995**, *67*, 183.
- (35) (a) Sancar, A. *Annu. Rev. Biochem.* **2000**, *69*, 31. (c) Sancar, A. *Chem. Rev.* **2003**, *103*, 2203.
- (36) (a) Ziegler, A.; Jonason, A. S.; Leffell, D. J.; Simon, J. A.; Sharma, H. W.; Kimmmerlman, J.; Remington, L.; Jacks, Y.; Brash, D. E. *Nature* **1994**, *372*, 773. (b) Kraemer, K. H. *Proc. Natl. Acad. Sci. U.S.A.* **1997**, *94*, 11.
- (37) (a) Taylor, J.-S. *J. Chem. Educ.* **1990**, *67*, 835. (b) Donahue, B. A.; Yin, S.; Taylor, J.-S.; Reines, D.; Hanawalt, P. C. *Proc. Natl. Acad. Sci. U.S.A.* **1994**, *91*, 8502.
- (38) Tommasi, S.; Swiderski, P. M.; Tu, Y.; Kaplan, B. E.; Pfeifer, G. P. *Biochemistry* **1996**, *35*, 15693.
- (39) Shindell, D. T.; Rind, D.; Lonergan, P. *Nature* **1998**, *392*, 589.
- (40) Aoki, S.; Sugimura, C.; Kimura, E. *J. Am. Chem. Soc.* **1998**, *120*, 10094.
- (41) Cadet, J.; Vigny, P. *Bioorganic Photochemistry*; Morrison, H., Ed.; John Wiley & Sons: New York, 1989; p 1.
- (42) (a) Kimura, E.; Ikeda, T.; Aoki, S.; Shionoya, M. *J. Biol. Inorg. Chem.* **1998**, *3*, 259. (b) Kimura, E.; Ikeda, T.; Shionoya, M. *Pure Appl. Chem.* **1997**, *69*, 2187.
- (43) Kimura, E.; Kitamura, H.; Ohtani, K.; Koike, T. *J. Am. Chem. Soc.* **2000**, *122*, 4668.
- (44) (a) Eichhorn, G. L. *Nature* **1962**, *194*, 474. (b) Venner, H.; Zimmer, C. *Biopolymers* **1996**, *4*, 321–335. (c) Dove, W. F.; Davidson, N. N. *J. Mol. Biol.* **1962**, *5*, 467.
- (45) (a) van Dyke, M. W.; Dervan, P. B. *Nucleic Acid Res.* **1983**, *11*, 5555. (b) van Dyke, M. W.; Dervan, P. B. *Science* **1984**, *225*, 1122. (c) van Dyke, M. W.; Hertsberg, R. P.; Dervan, P. B. *Proc. Natl. Acad. Sci. U.S.A.* **1982**, *79*, 5470.
- (46) (a) Chu, W.; Shinomiya, M.; Kamitori, K. Y.; Kamitori, S.; Carlson, R. G.; Weaver, R. F.; Takusagawa, F. *J. Am. Chem. Soc.* **1994**, *116*, 7971. (b) Wittung, P.; Nielsen, P. E.; Buchardt, O.; Egholm, M.; Norden, B. *Nature* **1994**, *368*, 561.
- (47) Kikuta, E.; Murata, M.; Katsube, N.; Koike, T.; Kimura, E. *J. Am. Chem. Soc.* **1999**, *121*, 5426.
- (48) Kikuta, E.; Koike, T.; Kimura, E. *J. Inorg. Biochem.* **2000**, *79*, 253.
- (49) Kikuta, E.; Katsube, N.; Kimura, E. *J. Biol. Inorg. Chem.* **1999**, *4*, 431.
- (50) Kikuta, E.; Matsubara, R.; Katsube, N.; Koike, T.; Kimura, E. *J. Inorg. Biochem.* **2000**, *82*, 239.
- (51) (a) Coll, M.; Frederick, C. A.; Wang, A. H. J.; Rich, A. *Proc. Natl. Acad. Sci. U.S.A.* **1987**, *84*, 8385. (b) van Dyke, M. W.; Hertsberg, R. P.; Dervan, P. A. *Proc. Natl. Acad. Sci. U.S.A.* **1982**, *79*, 5470.
- (52) (a) Trotta, E.; D'Ambrosio, E.; Del Grosso, N.; Ravagnan, G.; Cirilli, M.; Paci, M. *J. Biol. Chem.* **1993**, *268*, 3944. (b) Griffin, J. H.; Dervan, P. B. *J. Am. Chem. Soc.* **1987**, *109*, 6840.
- (53) Bailly, C.; Hamy, F.; Waring, M. J. *Biochemistry* **1996**, *35*, 1150.
- (54) (a) Portugal, J.; Waring, M. J. *Biochim. Biophys. Acta* **1988**, *949*, 158. (b) Fox, K. R.; Waring, M. J. *Biochim. Biophys. Acta* **1987**, *909*, 145. (c) Drew, H. R. *J. Mol. Biol.* **1984**, *176*, 535.
- (55) Bucher, P. *J. Mol. Biol.* **1990**, *212*, 563.
- (56) Sharp, P. *Cell* **1992**, *68*, 819.
- (57) Bellorini, M.; Moncollin, V.; D'Incalci, M.; Mongelli, N.; Manto-vani, R. *Nucleic Acids Res.* **1995**, *23*, 1657.
- (58) Kikuta, E.; Aoki, S.; Kimura, E. *J. Biol. Inorg. Chem.* **2002**, *7*, 473.
- (59) (a) Martin, J. C. *Nucleotide analogues as antiviral agents*; American Chemical Society: Washington, D.C., 1989. (b) Huryn, D. M.; Okabe, M. *Chem. Rev.* **1992**, *92*, 1745. (c) De Clercq, E. *J. Med. Chem.* **1995**, *38*, 2491.
- (60) Zimmerman, T. P.; Mahony, W. B.; Prus, K. L. *J. Biol. Chem.* **1987**, *262*, 5748.
- (61) (a) Mitsuya, H.; Broder, S. *Nature* **1987**, *325*, 773. (b) Bourdais, J.; Biondi, R.; Sarfati, S.; Guerreiro, C.; Lascu, I.; Janin, J.; Véron, M. *J. Biol. Chem.* **1996**, *271*, 7887.
- (62) Aoki, S.; Honda, Y.; Kimura, E. *J. Am. Chem. Soc.* **1998**, *120*, 10018.
- (63) (a) Kimura, E.; Aoki, S. *J. Am. Chem. Soc.* **1997**, *119*, 3068. (b) Kimura, E.; Koike, T.; Aoki, S. *J. Synth. Org. Chem., Jpn.* **1997**, *55*, 1052. (c) Aoki, S.; Iwaida, K.; Hanamoto, N.; Shiro, M.; Kimura, E. *J. Am. Chem. Soc.* **2002**, *124*, 5256. (d) Kimura, E.; Gotoh, T.; Aoki, S.; Shiro, M. *Inorg. Chem.* **2002**, *41*, 3239.
- (64) Aoki, S.; Kimura, E. *J. Am. Chem. Soc.* **2000**, *122*, 4542.
- (65) Aoki, S.; Kimura, E. *Rev. Mol. Biotechnol.* **2002**, *90*, 129.
- (66) Furman, P. A.; Fyfe, J. A.; St. Clair, M. H.; Weinhold, K.; Rideout, J. L.; Freeman, G. A.; Lehrman, S. N.; Bolognesi, D. P.; Broder, S.; Mitsuya, H.; Barry, D. W. *Proc. Natl. Acad. Sci. U.S.A.* **1986**, *83*, 8333.
- (67) Magnani, M.; Casabianca, A.; Fraternali, A.; Brandi, G.; Ges-sani, S.; Williams, R.; Giovine, M.; Damonte, G.; De Flora, A.; Benatti, U. *Proc. Natl. Acad. Sci. U.S.A.* **1996**, *93*, 4403.
- (68) Aoki, S.; Honda, Y.; Kimura, E. Unpublished results.
- (69) (a) Inouye, Y.; Kanamori, T.; Yoshida, T.; Bu, X.; Shionoya, M.; Koike, T.; Kimura, E. *Biol. Pharm. Bull.* **1994**, *17*, 243. (b) Inouye, Y.; Kanamori, T.; Sugiyama, M.; Yoshida, T.; Koike, T.; Shionoya, M.; Enomoto, K.; Suehiro, K.; Kimura, E. *Antiviral Chem. Chemother.* **1995**, *6*, 337. (c) Inouye, Y.; Kanamori, T.; Yoshida, T.; Koike, T.; Shionoya, M.; Fujioka, H.; Kimura, E. *Biol. Pharm. Bull.* **1996**, *19*, 456.
- (70) (a) Bridger, G. J.; Skerlj, R. T.; Padmanabhan, S.; Martellucci, S. A.; Henson, G. W.; Struyf, S.; Witvrouw, M.; Schols, D.; De Clercq, E. *J. Med. Chem.* **1999**, *42*, 3971. (b) Gerlach, L. O.; Skerlj, R. T.; Bridger, G. J.; Schwartz, T. W. *J. Biol. Chem.* **2001**, *276*, 14153.
- (71) Liang, X.; Parkinson, J. A.; Weishäupl, M.; Gould, R. O.; Paisey, S. J.; Park, H.-S.; Hunter, T. M.; Blindauer, C. A.; Parson, S.; Sadler, P. J. *J. Am. Chem. Soc.* **2002**, *124*, 9105.
- (72) Hermann, T. C. *Angew. Chem., Int. Ed. Engl.* **2000**, *39*, 1890.
- (73) (a) Mayhood, T.; Kaushik, N.; Pandey, P. K.; Kashanchi, F.; Deng, L.; Pandey, V. N. *Biochemistry* **2000**, *39*, 11532. (b) Mei, H.-Y.; Galan, A. A.; Halim, N. S.; Mack, D. P.; Morelan, D. W.; Sanders, K. B.; Truong, H. N.; Czarnik, A. W. *Bioorg. Med. Chem. Lett.* **1995**, *5*, 2755. (c) Sucheck, S. J.; Wong, A. L.; Koeller, K. M.; Boeher, D. D.; Draker, K.; Sears, P.; Wright, G. D.; Wong, C.-H. *J. Am. Chem. Soc.* **2000**, *122*, 5230. (d) Sucheck, S. J.; Wong, A. L.; Koeller, K. M.; Boeher, D. D.; Draker, K.; Sears, P.; Wright, G. D.; Wong, C.-H. *J. Am. Chem. Soc.* **2000**, *122*, 5230.
- (74) (a) Mazumder, A.; Chan, C. H. B.; Gaynor, R.; Sigman, D. S. *Biochem. Biophys. Res. Commun.* **1992**, *187*, 1503. (b) Cheng, C. H.; Kuo, Y. N.; Chuang, K. S.; Luo, C. F.; Wang, W. *J. Angew. Chem., Int. Ed. Engl.* **1999**, *38*, 1255.
- (75) Jones, K. A.; Peterlin, B. M. *Annu. Rev. Biochem.* **1994**, *63*, 717.
- (76) Kikuta, E.; Aoki, S.; Kimura, E. *J. Am. Chem. Soc.* **2001**, *123*, 7911.
- (77) (a) Aoki, S.; Shiro, M.; Koike, T.; Kimura, E. *J. Am. Chem. Soc.* **2000**, *122*, 576. (b) Aoki, S.; Shiro, M.; Kimura, E. *Chem. Eur. J.* **2002**, *8*, 929. (c) Aoki, S.; Zulkefeli, M.; Shiro, M.; Kimura, E. *Proc. Natl. Acad. Sci. U.S.A.* **2002**, *99*, 4894.

CR020617U

